28. *Supplementary Study on the Stereometrical Distribution of the After-shocks of the Great Tango Earthquake of 1927.*

By Nobuji NASU,

Earthquake Research Institute.

(Received March 20, 1935.)

Introduction. Since the publication in 1929 of our paper[1] relating to the stereometrical distribution of the seismic foci of the Tango after-shocks, data have been obtained necessitating certain revisions and additional comments. The object of this paper is to describe and discuss such revisions and additional facts so as to bring the paper up to date,

(1) It was found that the values of k, the constant factor in the formula $D=kt$, which were determined graphically and listed in TABLE IV of our first paper should have been extended to the second decimal place to be sufficient for determining the seismic focus. In working out the value of k graphically, however, we found that the figures from the second (inclusive) after the decimal were not reliable, This value differ slightly with every trial determination, which is doubtless on account of errors that creep in when drawing the figures on a map. In these circumstances, the values of k in the present study were determined throughout by calculations, instead of by the graph method. In these calculations the number of the selected earthquakes was increased from 8 to 9. The mean value of k thus determined came out as 8·40, differing but slightly from 8·41 as given in our former paper; a difference of only 0·01. In this paper the value of k has been taken as 8·40. The formula for k is moreover slightly corrected by inserting the correct values of the distances between the seismological stations as well as the coordinates of the stations. For convenience, the table containing the determined k is specified in this paper by the same serial numbers as those in the former report, which is TABLE IV in this paper. And since there is no means by which

1) N. NASU, "A Stereometrical Study of the After-shocks of the Great Tango Earthquake with Special Reference to the Mechanism of their Occurrence", *Journ. Facult. Sc.*, [ii], **3** (1929), 29.

2) *Journ. Facult. Sc., loc. cit.* p. 38, Table v.

we can ascertain the durations of the preliminary tremors at stations that are not included in our network of observations, it is not possible to say that the values of k given in the next table (TABLE V)[2] in the previous paper are correct. For this reason, TABLE V is not included in this paper.

(2) In the present study, the seismic foci were accurately determined from observations made at either three of four stations. There being about 30 foci in our previous study that cannot be regarded as being accurate, these are excluded from the present paper.

(3) The errors in the position of the seismic foci are now calculated to a sufficient extent to enable discussion of the arrangement of the seismically weak zones or fault planes from which the aftershocks originated. In the APPENDIX[3] will be found the calculations of the errors mentioned.

(4) In the diagrams (Figs. 24~33) in our previous paper, showing the vertical distribution of the seismic foci are drawn too many lines on which the foci of shocks are shown to be grouped, included in which are, however, several lines whose distance from the next line does not exceed 2 or 3 km. The actual existence of such planes as indicated by these lines becomes doubtful, were the errors in the seismic foci due to errors in observation taken into consideration. But, on the other hand, however, there is no reason to regard the whole of our previous results as being in error on this account. It must be understood therefore that the lines, or planes, which were determined by projecting the seismic foci to certain vertical plane were merely drawn in certain directions because they were the only directions in which it was possible to draw them from our studies of the disposition of the seismic foci In the present study, an attempt has been made to determine only such conspicuous seismically weak zones as are most likely to exist in reality (Figs. 25~56). Possible errors in the position of the seismic foci are now also taken into consideration. The number of the weak zones, or fault planes, thus determined are less than that determined in our previous study.

(5) Another improvement is that the classification of the seismic foci according to the times in which the earthquakes occurred receives more attention in this paper than it did in the previous one, with the result that the migration of the seismically active centre with time can be illustrated more conveniently than it was possible before.

Lastly, it must be borne in mind that the new treatment of the

3) This APPENDIX is published in the *Jap. Journ. Astr. Geophys.*, **12** (1935).

subject in no way affects the general results that were obtained in the case of our previous study.

Determination of k *in the formula for the computation of focal distance by means of the duration of preliminary tremors.*

It is assumed that the four stations, Maiduru, Kinosaki, Kôbe-mura, Taiza, lie on a horizontal plane, $Z=0$. Let the X and Y axes be horizontal, see Figs. 8, and the origin of coordinates be taken at any of the stations, say, Maiduru. Let the X axis be taken on the straight line joining Maiduru and Kinosaki; assuming the northwest as its positive sense. Let the Y axis be taken perpendicular to the former axis with the northeast as its positive sense. Let the coordinates of the four stations be (0, 0, 0), (x_1, 0, 0), (x_2, y_2, 0) and (x_3, y_3, 0), respectively.

Assuming now that the focus lies at a point whose coordinates are (X, Y, Z), we get the following relations for the focal distances of the four stations;

$$D_0=\sqrt{X^2+Y^2+Z^2}=kt_0,$$

$$D_1=\sqrt{(X-x_1)^2+Y^2+Z^2}=kt_1,$$

$$D_2=\sqrt{(X-x_2)^2+(Y-y_2)_2+Z_2}=kt_2,$$

$$D_3=\sqrt{(X-x_3)^2+(Y-y_3)^2+Z^2}=kt_3,$$

where D_0, D_1, D_2, D_3 are the focal distances of the four stations, and t_0, t_1, t_2 and t_3 are the durations of the preliminary tremors at the respective stations.

Solving the simultaneous equations in X, Y, Z and k, we have four expressions, of which the one for the constant factor k is

$$k=\sqrt{\frac{(x_3y_2-x_2y_3)\,d_1^2-(d_3^2y_2-d_2^2y_3)\,d_1}{(x_3y_2-x_2y_3)\,\tau_1+(y_3\tau_2-y_2\tau_3)\,d_1}},$$

where d_1, d_2, d_3 are the respective distances from Maiduru, of Kinosaki, Kôbe-mura and Taiza; and $\tau_1=t_0^2-t_1^2$, $\tau_2=t_0^2-t_2^2$, $\tau_3=t_0^2-t_3^2$. For

4) The numerical values here adopted were determined in the topographical maps of Miyadu and Tottori, scale 1/200,000. Some of the numerical values slightly differ from those which were used in our previous paper, and which are now corrected.

our network of stations, the following numerical values[4] are required in the reduction of the expression for k.

$$d_1=50{\cdot}4 \text{ km.} \quad x_1=50{\cdot}4 \text{ km.}$$

$$d_2=27{\cdot}0 \text{ km.} \quad x_2=25{\cdot}8 \text{ km.} \quad y_2=7{\cdot}9 \text{ km.}$$

$$d_3=38{\cdot}3 \text{ km.} \quad x_3=31{\cdot}9 \text{ km.} \quad y_3=21{\cdot}2 \text{ km.}$$

Inserting the above given values, the expression for k becomes

$$k=\sqrt{\frac{554355{\cdot}2}{375{\cdot}4t_0^2+295{\cdot}0t_1^2-1068{\cdot}5t_2^2+398{\cdot}2t_3^2}},$$

During a period of about six months after the installation of the second network of stations, there were nine after-shocks for which the seismic foci, as well as the above-mentioned factor could be determined.

By using the formula we calculated the values of k to the second decimal place; the accuracy being sufficient for our present purpose. The values of k are shown in Table IV.

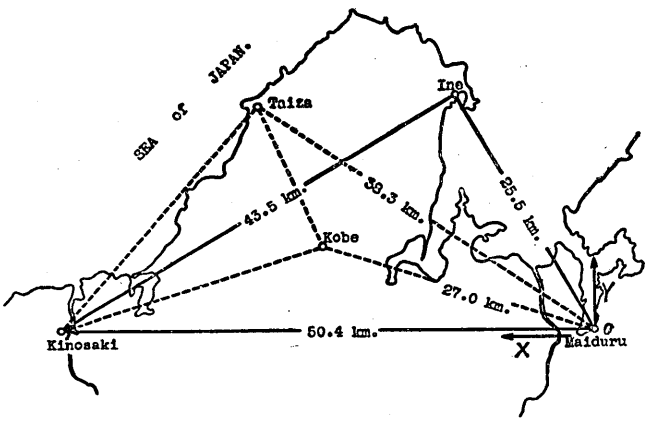

Fig. 8. Networks of the Seismological Stations.
——— the first network.
..... the second network.

The values of k obtained in the Tango after-shocks came out as 8·40 in its mean value.

Table IV. Durations of the Preliminary Tremors, Values of k and Focal Depths of the Earthquakes.

Time of earthquake occurrence.				Duration of the preliminary tremors.				Factor k	Focal depth
				Maiduru	Kinosaki	Kôbe	Taiza		
Month	Day	h	m	sec.	sec.	sec.	sec.		km.
I	30,	5	01	2·5	3·6	1·4	3·0	8·51	6·0
I	30,	18	41	5·1	2·8	2·3	1·7	8·55	12·2
II	12,	21	27	5·0	3·0	2·2	1·6	8·38	12·0
II	14,	20	48	4·0	2·8	1·7	2·8	8·15	11·2
II	18,	18	49	5·0	2·6	2·3	2·4	8·31	14·8
II	19,	5	27	3·3	3·3	1·2	2·0	8·68	10·3
II	29,	10	38	3·2	3·6	2·0	3·3	8·47	13·8
III	1,	22	34	5·5	2·0	2·7	2·9	8·28	13·9
VI	16,	12	06	3·0	3·5	0·9	2·2	8·30	6·7

Distribution of the epicentres of the Tango after-shocks.

During our observations, lasting about $1\frac{1}{2}$ years, the after-shocks recorded at least at one of our stations totaled 1307, and we were able to determine accurately the seismic foci of 446 shocks. Although, in our previous paper,[5] 482 determined foci were reported, among them were about 30 foci that we believe are not so accurate, owing to lack of sufficient observations at one of the stations forming the necessary three. The positions of these foci were determined from the durations of the preliminary tremor and the directions of initial motion at the remaining two stations. In this paper, such foci are excluded. There were several more earthquakes in which the duration of the preliminary tremor at one station exceeded 8·0 sec., so that the positions of the seismic origins determined were not so accurate as those of earthquakes with shorter durations of preliminary tremors. In this paper, therefore these earthquakes are also excluded. There are also a few after-shocks that are excluded or newly added for other reasons.

The positions of the seismic foci were determined mainly graphically, using maps of scales 1/200,000 and 1/400,000. The distances of stations composing the networks are shown in Fig. 8. The horizon-

5) N. NASU, "A Stereometrical Study of the After-shocks of the Great Tango Earthquake with Special Reference to the Mechanism of their Occurrence", *Journ. Facult. Sc.*, [ii], **3** (1929), 29.

tal axes of coordinates were taken in the directions as shown in the same figure, while the positions of the seismic origins were expressed by coordinates X, Y, Z; the Z axis being taken downward in its positive sense.

The seismic foci of 446 shocks were determined by seismic triangulation, of which 9 were observed from four stations. In these 9 latter earthquakes, the foci were determined by using the values of k, specially determined for each earthquake and not by mean value, $k=8{\cdot}4$.

A few words are necessary regarding the case $Z=0$. When $Z=0$, the three circles drawn with each station as centre generally intersect at a point. Sometimes the arcs thus described merely enclose a circular-arc-triangle. When this circular-arc-triangle could be obtained we assumed that the epicentre lay at the approximate centre of this triangle, and determined the coordinates of this centre. Another cases of $Z=0$, although very rare, is that in which the circles do not intersect, in which case the position of the seismic foci were determined in the following mannner: Assuming the observed values of the preliminary tremor to be smaller than the actual by a certain amount of error, we made corrections for the radii of the circles. The time error was assumed to be 0·1 sec. If the circles having these corrected radii enclosed a circular-arc-triangle, the position of the seismic focus could be determined, otherwise it was impossible.

We must next bear in mind the accuracy in the graphical determination of the seismic focus. The values of X, Y, Z given in Table VI having been determined graphically they, naturally, contain certain errors that crept in when drawing the figures on the maps. The errors in the coordinates, however, were in most cases within about $\pm 0{\cdot}2$ km. when a map of scale 1/200,000 was used, and within about $\pm 0{\cdot}4$ km. in the case of a map of scale 1/400,000; these amounts of errors correspond to 1 mm. on the respective maps, and are the probable error from this source. Thus, the fractions of a kilometer in the values of X, Y, Z in Table VI are not accurate within the errors mentioned, which however do not affect our present study. As a matter of fact, fractions of a kilometer in the coordinates of the seismic focus are not worth troubling about.

Distributions of the epicentres of the after-shocks are shown in Figs. 9~15.

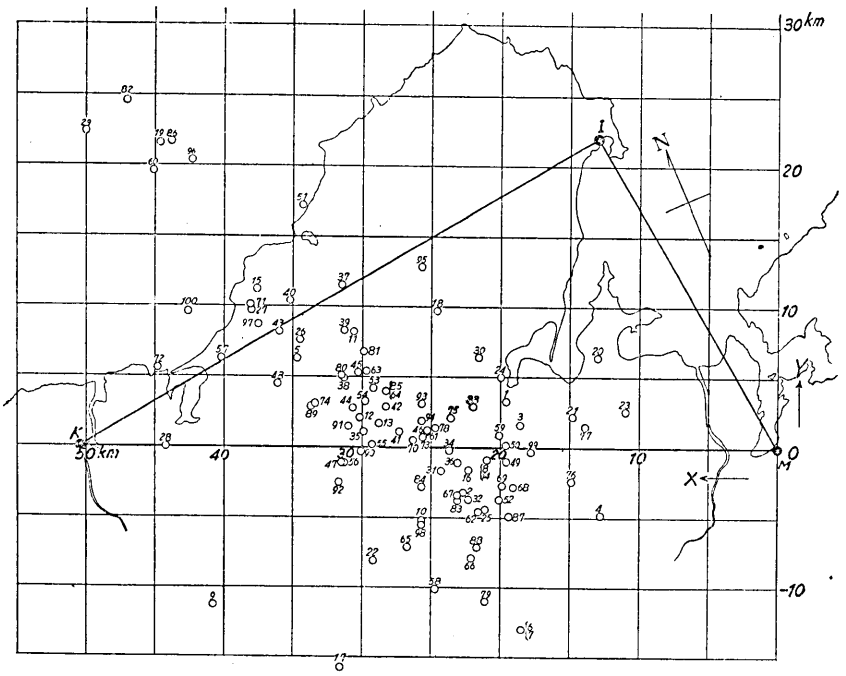

Fig. 9. Map showing the distribution of the epicentres for the period March 12~17, 1927.

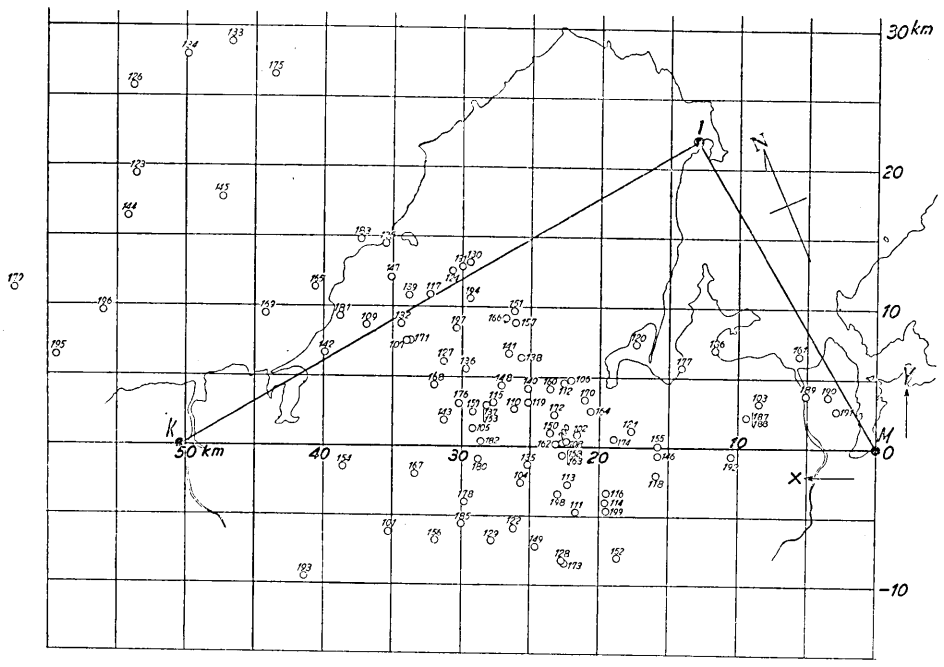

Fig. 10. Map showing the distribution of epicentres for the period March 17~April 1, 1927.

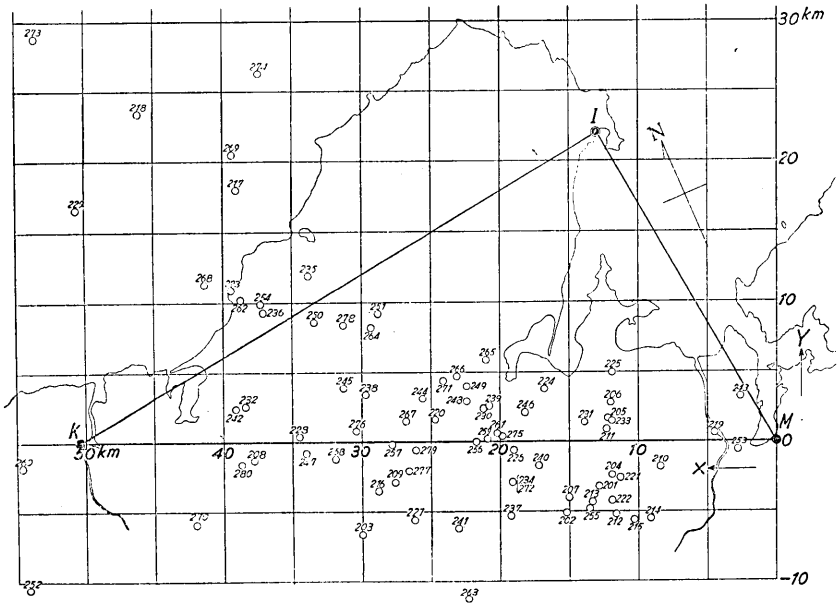

Fig. 11. Map showing the distribution of the epicentres for the period April 1~30, 1927.

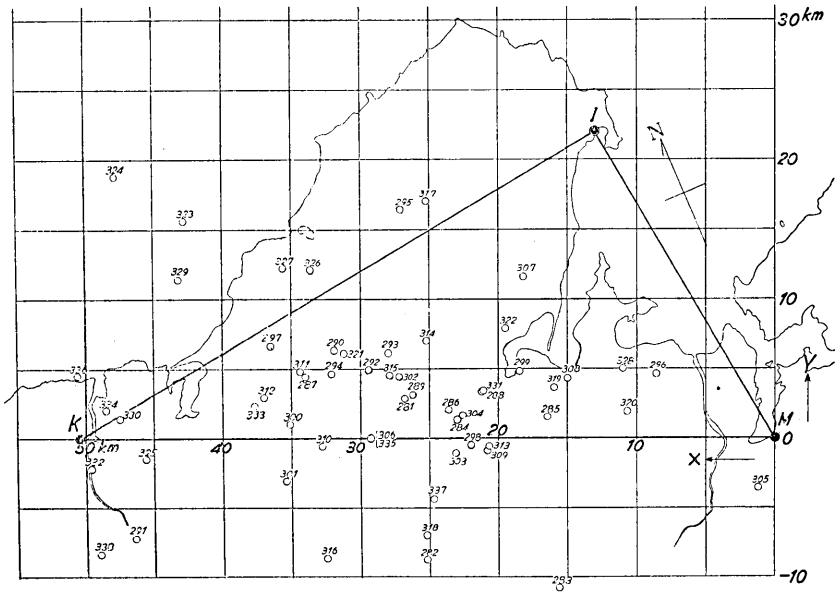

Fig. 12. Map showing the distribution of the epicentres for the period May 1~31, 1927.

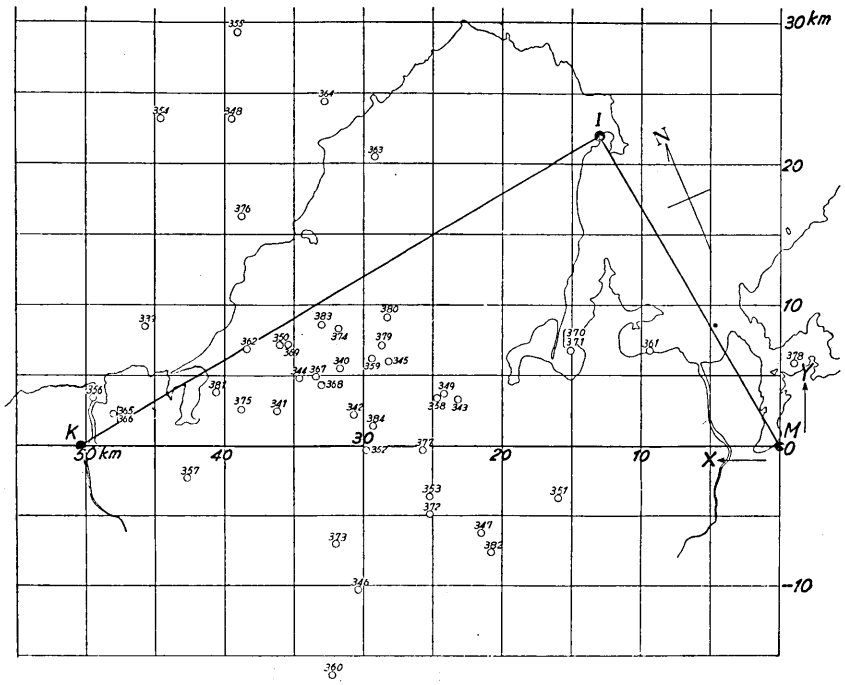

Fig. 13. Map showing the distribution of the epicentres for the period June 1~August 31, 1927.

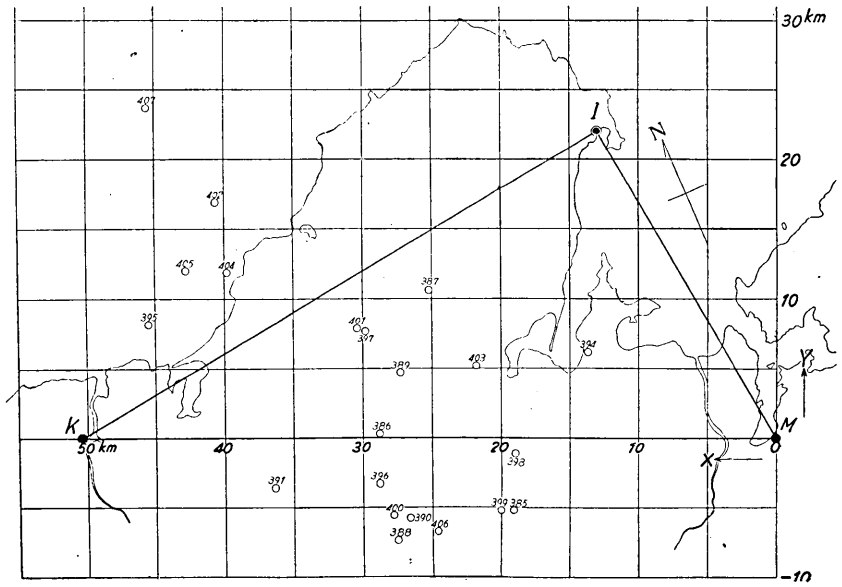

Fig. 14. Map showing the distribution of the epicentres for the period Sept. 1~Dec. 31. 1927.

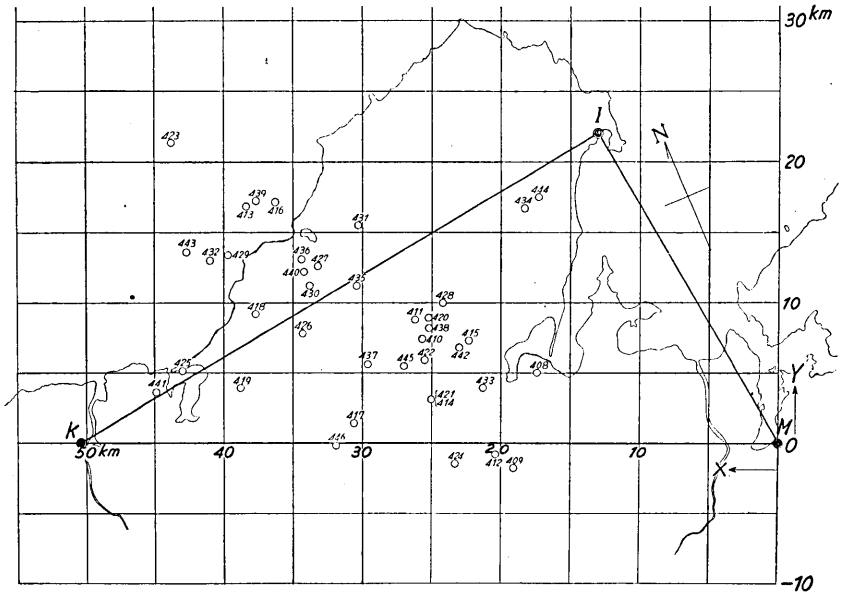

Fig. 15. Map showing the distribution of the epicentres for the period January 1~July 15, 1928.

Distribution of the after-shocks in a vertical plane: stereometrical distribution of the seismic foci of the after-shocks.

A perusal of the history of seismological research in this country will show that instrumental records of after-shocks were first obtained in the case of the great Mino-Owari earthquake of 1891.[6] Thenceforward, observations of after-shocks became an established feature with every visitation of a destructive earthquake.

Much study has been expended on the phenomena of after-shocks, but they have mainly been in the direction of statistics. As the results of his experimental studies on the elasticity and rigidity of rocks, the late Prof. S. Kusakabe[7] deduced a formula based on the time-frequency curve of after-shocks. His investigations have been satisfactory so far as concerned the interpretation of the frequency of after-shocks, but they were not extended to embrace the space distribution of after-shocks. Actually, the problem of space distribution of after-

6) D. KIKUCHI, Recent Seismological Investigation in Japan, 1904.

7) S. KUSAKABE, "Modulus of Elasticity of Rocks and Velocities of Seismic Waves with a Hint to the Frequency of After-shocks." *Publ. Earthq. Inv. Comm.*, **17** (1904).

shocks is one that has, so far, scarcely received the attention of investigators.

There are two different theories regarding the generation of earthquakes. The one is that an earthquake takes place as an accompaniment to the movement of earth-blocks, and the other is that the earthquake is caused by acute movements of magma.

According to the former theory, the generation of after-shocks may be explained as follows: following a great earthquake we may expect the occurrence of a number of after-shocks about the disturbed area, each of which after-shocks may be supposed to have removed a source of instability from under our feet. If this were a block movement, then once a great earthquake takes place as an accompaniment to this movement, the disturbance, that is, the block movement ought to continue. The direction of this movement will be, not only along the principal fault, but may also follow the course of some minor faults as well. The underground block will moreover be broken up into innumerable smaller blocks, not only by the principal fault, but also by countless minor faults. In these circumstances, it is not difficult to conceive of these small blocks also moving along the minor faults. With every energetic movement of such blocks, earthquakes are bound to occur at their bounding surface.

According to the second theory, while the first big earthquake is generated by certain acute movements of magma, the after-shocks are due to its residual or renewed movement about the originally disturbed area.

Though these two theories differ as to the generation mechanism of earthquakes, on one point they agree, and that is that the earthquakes are liable to originate in weak zones in the earth's crust, such as fault planes. From the foregoing it naturally follows that after-shocks might originate in the principal faults, or in the minor faults contiguous to them. Such fault planes are, however easily traced by a careful study of the distribution of the seismic foci.

Before proceeding further, a few words might be said by way of explanation regarding the Gômura fault zone. This fault zone consisted of five main segments[8] arranged *en échelon*, the *échelon* in this case, to use Prof. Fujiwhara's nomenclature,[9] being "negative"; that

8) N. YAMASAKI and F. TADA, "The Oku-Tango Earthquake," *Bull. Earthq. Res. Inst.*, **4** (1928), 159.

9) S. FUJIWHARA, "On the *èchelon* Structure of Japanese Volcanic Ranges and its Significance from the Vortical Point of View," *Gerl. Beitr. zur Geophys.*, **16** (1927), 1.

is to say, each segment ran in the second and fourth quadrants when the abscissa was taken coincident with the main trend of the fault zone. This condition manifested itself in the southern part of the Gômura fault zone, but not in the northern. As a probable explanation of this singularity, Prof. Imamura[10] drew attention to the possible difference in the stress distribution between the northern and southern blocks lying west of the Gômura fault, adding, that if such was the case, the stress in the northern block might have been applied in a direction almost perpendicular to the fault, and in the southern part in a direction parallel with the fault.

Here it may not be irrelevant to make a little digression and refer to the experiments made some time ago by Prof. Fujiwhara[11] with the purpose of studying the precise manner of crack-formation. Forces were applied to models made of various substances, and the results showed that with substance feebly resistant to tensional forces, parallel cracks developed obliquely to the line of shear; whereas with substances feebly resistive to bending forces, a group of carcks formed athwart the tensional force. Subjection of the models to uniform tension or compression resulted in the developement one after another of two kinds of cracks, quite regardless of the substance tested, viz., tension cracks and compression cracks. As to these two modes of cracking, those of secondary formation always lay in a direction symmetrical to the primary cracks. To illustrate, if the primary cracks were at an angle of 45°, as would be the case with an isotropic, homogeneous substance, then the secondary cracks developed perpendicularly to the primary cracks. From this it may be inferred that there were many other faults near the principal ones that came into existence with the present earthquake.

The following will illustrate the methods adopted by the writer in studying the positions of seismic foci. As will be evident from the distribution of the fault lines (Fig. 24), the land mass in the Tango seismic area may be divided into a number of small blocks with the faults as the boundaries of their upper surfaces. Though the actual blocks in nature are not regular geometrical figures, we could roughly divide the Tango seismic area into four large blocks as shown in Fig. 24. The boundaries of these blocks are nearly parallel to the predominant faults, such as the Gômura fault, for example. We shall

10) A. IMAMURA, "On the Destructive Tango Earthquake on March 7, 1927," *Bull. Earthq. Res. Inst.*, **4** (1928), 179.

11) S. FUJIWHARA, "Torsional Form on the Earth Surface and the Great Earthquake of Sagami Bay," *Kisyô Syûsi*, [ii], **2~1** (1924).

then project the seismic foci in each block on certain vertical planes. For example, we shall take a crustal block No. III, which is bounded by the Gômura fault on the east and by a line nearly parallel to the Yamada fault (the X' axis in Fig. 24) on the south, and project all the foci in this block on a vertical plane normal to the Gômura fault zone, arranging the foci of the shocks according to the times of their occurrence. In our former studies[12] of disposition of the seismic foci of the Tango after-shocks, the foci were classified into the following three classes:

(1) The foci of the first class, such as those of shocks that occurred early, that is, during a period of about 50 days following the great earthquake, and marked in the diagrams by dots.

(2) The foci of the second class, such as those of shocks that occurred in the next period, that is, during the period from the end of April to the end of August of 1927, and marked by crosses.

(3) The foci of the third class, such as those of shocks that occurred during a period of about eleven months from the beginning of September, 1927, to the end of July the next year, and marked by asterisks.

Upon classifying the foci in this way it was found that they showed quite different positions according to the times of occurrence of the respective earthquakes. But since then it was found convenient in studying the disposition of the foci to arrange them in more classes than the three just mentioned. By doing so, the change in positions of seismically active centres with time could be more clearly shown than could be done heretofore. Thus, in the present study, the foci were divided into several classes according to the times in which the earthquakes occurred, and for each class of foci the distributions of the seismic foci shown in different diagrams. From these diagrams the migrations of the seismically active centres could be clearly studied.

Needless to say, the foci belonging in one class must be sufficiently numerous to enable us to correctly determine the mean position of the seismically active centre. For this reason, at least ten foci belonging in one class were taken.

It will be noticed that some of the foci projected in the above-stated manner may be grouped together into a number of systems of finite lines (foci lying on the same line being generally of the shocks that occurred successively), that are usually nearly parallel to each other. Here it must be remembered that the lines and planes refer-

12) N. NASU, "A Stereometrical Study of the After-shocks of the Great Tango Earthquake," *Journ. Facult Sc.*, [ii], **3** (1929), 29.

red to in this paper are not the lines and planes as understood in geometry. They are merely imaginary lines or planes in which the seismic foci lie, hence may not be straight, but assume any irregular form. Thus, as a matter of expediency the lines or planes deduced in the present study are indicated in the diagram by means of smooth curves or straight lines on which the foci are supposed to lie. It must further be understood that the lines as determined from the disposition of the foci show only the mean position of the seismically active zones or planes.

In taking the plane of projection parallel to the Gômura fault (the plane in this case being perpendicular to the former plane of projection) a new result is obtained again for the foci in the same block. Thus, in our studies the planes of projection were taken such that the one plane is parallel to the major geomorphologic faults and the other perpendicular to the same faults.

As the errors in the position of the seismic focus become fairly large if the focal depth were to exceed 25 km., particularly the errors in the horizontal directions, foci of such shocks as were deeper than 25 km. were excluded from our present studies.

We shall now consider the block that lies west of the Gômura fault zone.

Block No. III.

The surface of this block is bounded by those two conspicuous faults, the Cômura fault on the east and by the Yamada fault on the south. We studied not only seismic foci with their epicentres within the surface of this block, but also took into consideration foci in contiguous blocks, that is, the foci lying in a region designated as III in Fig. 24 were all studied.

(A) We shall first describe the shocks that occurred west of the Gômura fault zone. Most of the after-shocks that occurred during period March 12~15 (5~10 days after the great earthquake) had their origins west of the Gômura fault. The distribution of the epicentres of these shocks is shown in Fig. 25. In the case of 65 earthquakes, the seismic foci could be determined for this period, 39 of which were situated west of the Gômura fault or its extension as shown in the same figure. A notable fact is that these foci were in a zone running parallel to the Gômura fault; a zone of about $2\frac{1}{2}$ km. width. This zone is shown by the hatching area in Fig. 25. From this fact it will easily be seen that were weak zones or fault planes at certain depth, where particularly most of the after-shocks originat-

ed during the few days succeeding the great earthquake. For the

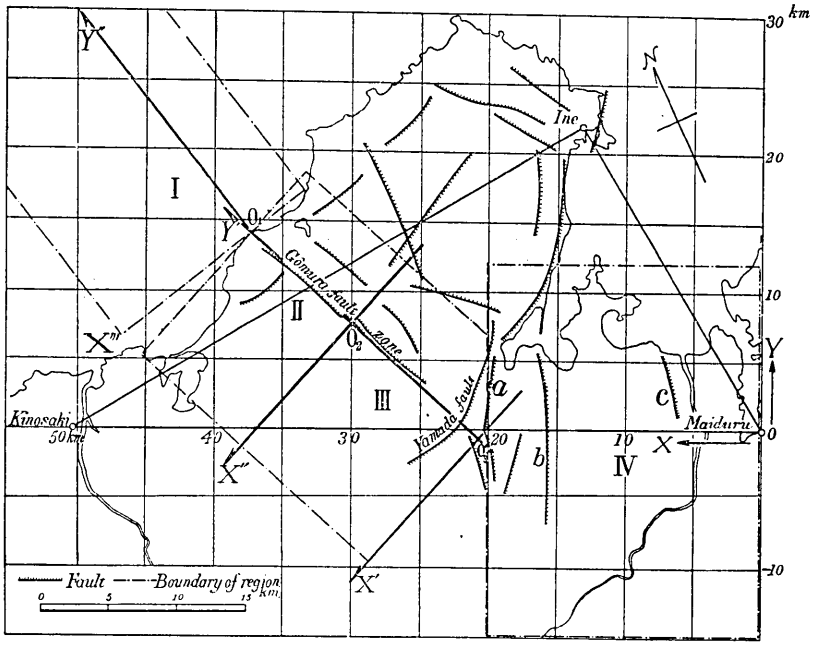

Fig. 24. Map showing the major geomorphologic faults in the Tango district and boundaries of regions which were taken for projections of seismic foci.

purpose of determining the depth of this weak zone, we shall project all the foci shown in Fig. 25 on a vertical plane parallel to the X' axis; the plane being nearly parallel to the trend of the Yamada fault. Let X' be the distance of the epicentres from the Y′ axis, which is assumed to be the mean trend of the Gômura fault: X' being positive southwestward and negative northeastward.

The values of X' of the epicentres of the after-shocks which are shown in Fig. 25 are given in Table VII.

Taking the values of X' as abscissa and the focal depth, Z, in Table VII as ordinate, the position of the foci in Fig. 25 are shown in Fig. 26, in which the black circles are the foci in region III and the white circles the foci lying outside of it.

It was found that the seismically weak zones in region III lay at a depth of about 15 km. As may be seen from Fig. 26, while the after-shocks in region III originated from depths of 13·5 km and 22·5 km, most of them were from depths exceeding 15 km, they being confined to a region bordered by the four lines, $Z=15$ km, $Z=20$ km,

$X'=0$ km, $X'=5$ km. It was also found that the earthquakes originated in the planes marked g_0 and h_0, although, as explained these planes are not strictly geometrical planes. Although the existence of plane g_0 is not so apparent from this figure compared with plane h_0, if we project the foci of the shocks that occurred during a period later than that now in question, then its existence becomes apparent as will be shown later.

We shall next take up the foci of the shocks that occurred during the period, March 15~31, 1927, and project them on the same vertical plane as before. (Fig. 27.) It will be seen from Fig. 27 that most of the foci were situated on the two sides of line h_0. It is noteworthy that another group of foci may be seen on line g_2. The presence of a seismically weak zone g_2 will become apparent upon projecting the foci of later shocks. It is probable that another group of foci exists at a depth of about 15 km. and also at a distance of about 5 km. west of the g_0-line, the zone marked g_1 in Fig. 27, although its existence is not positive as judged from the projection of the foci of the shocks that occurred in this period.

The foci of the shocks that occurred in the next period, April 1~30, do not show any remarkable features except that they were mostly distributed east of the line g_2, Fig. 28. Only two foci, No. 203 and No. 208, were situated west of the same line.

The foci of the after-shocks in May, 1927, may be grouped along two lines, h_1 and g_0, as shown in Fig. 29. Line h_1 shows the upper boundary of the seismically active region nearly parallel to line h_0, as already shown in Fig. 27. The position of line h_1, however is somewhat shallower than line h_0. It shows that the seismic activity migrated upward during this period. Of the foci that lie near line h_1, foci No. 300 and No. 310, may be grouped in line g_2 in Fig. 27, and the foci Nos. 337, 335 and 306 grouped in line g_1 in the same diagram. It is undeniable that the seismic activity was mainly confined to line g_0, which is seen to be in the same position as already determined in Fig. 26.

During the next period of three months, from June to August, 1927, the shocks were particularly active in a weak zone indicated by g_1. The distribution of the foci for this period is shown in Fig. 30. As to the distribution in this figure, no foci of shocks could be found on west side of line g_1.

Lastly, we shall take the foci of the shocks that occurred during the eleven months, from September 1927, to the middle of July 1928, and project them in the same manner as we have already done. We

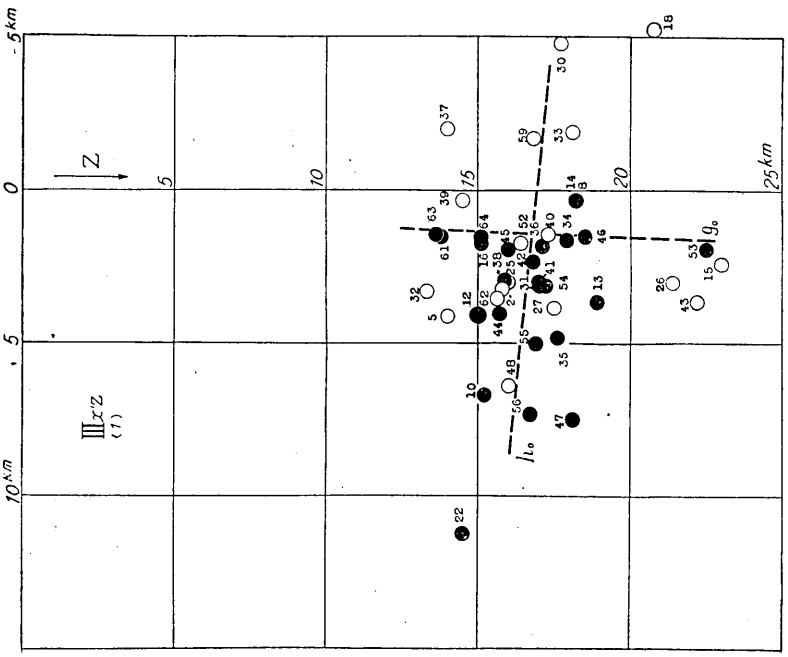

Fig. 26. Seismic foci lying in regions II, III, and environ projected on a vertical plane normal to the Gômura fault. (Distribution for the period, March 12~15, 1927.)
(Black circles are the seismic foci lying west of the Gômura fault and in region III.)

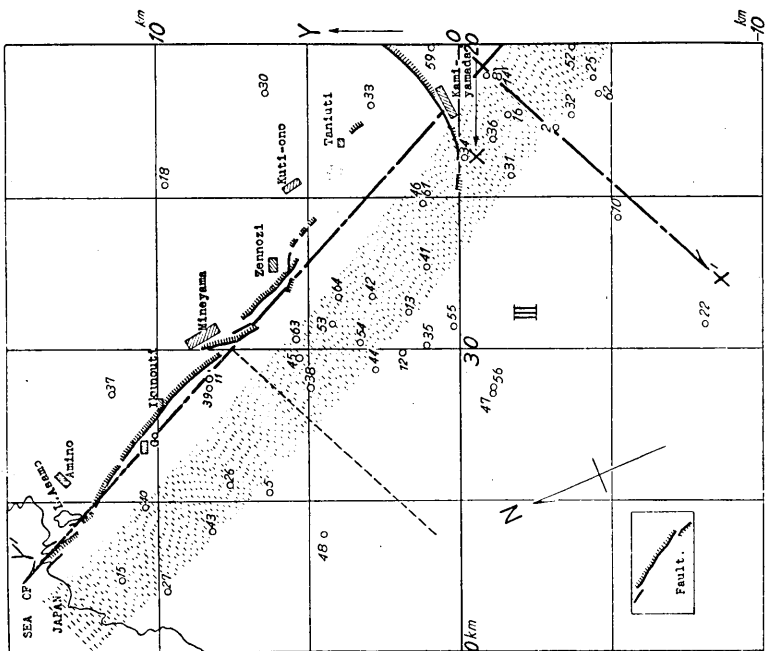

Fig. 25. Distribution of the epicentres of the after-shocks that occurred near the Gômura fault during a few days following the great earthquake of March 7, 1927.

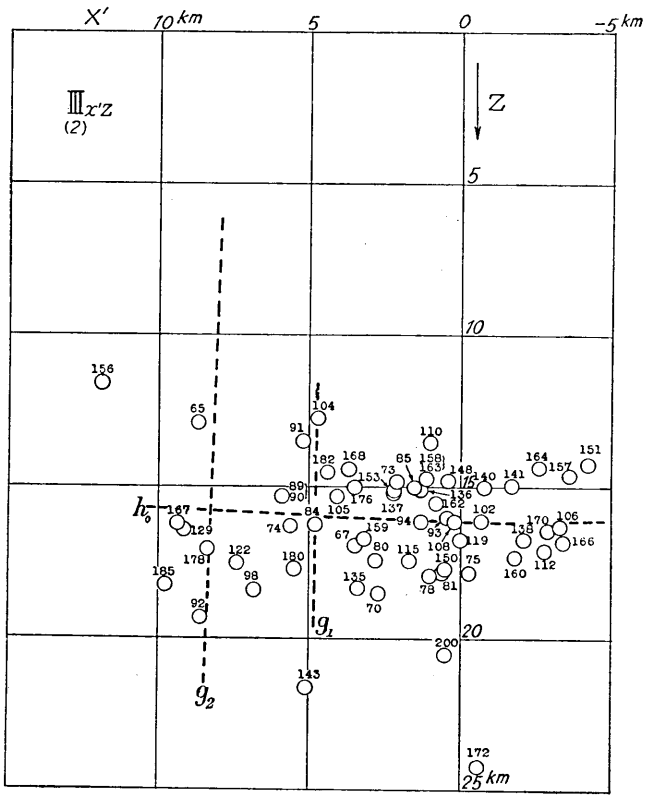

Fig. 27. Distribution of the seismic foci of the shocks that occurred during the period, March 15～April 1, 1927, on a vertical plane normal to the Gômura fault. (Region III.)

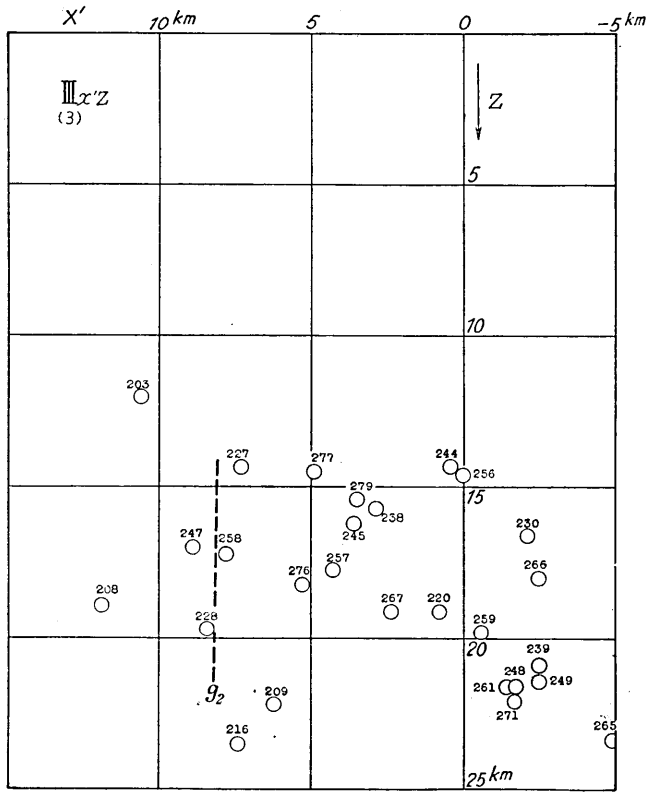

Fig. 28. Distribution of the seismic foci of the shocks that occurred during the period, April 1～30, 1927, on a vertical plane normal to the Gômura fault. (Region III.)

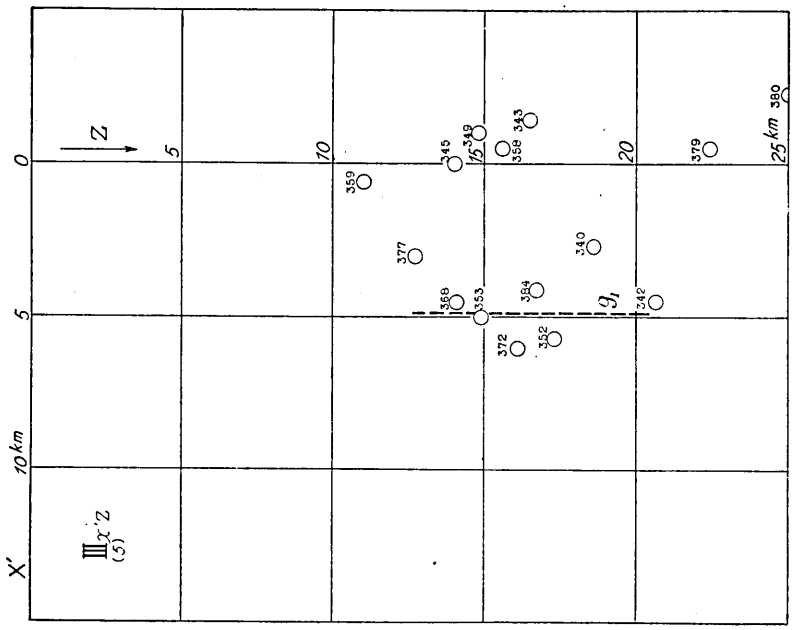

Fig. 30. Distribution of the seismic foci of the shocks that occurred during the period June 1～August 31, 1927, in a vertical plane normal to the Gômura fault. (Region III.)

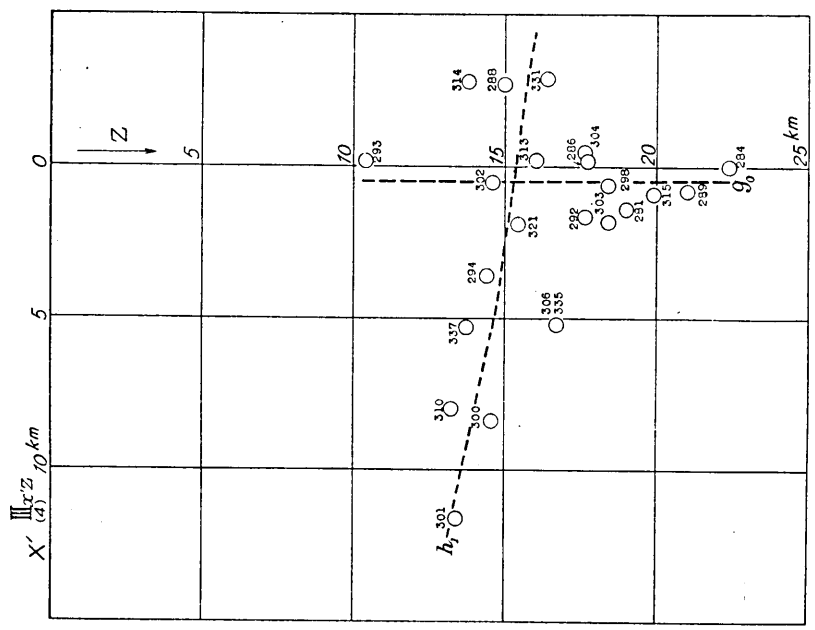

Fig. 29. Distribution of the seismic foci of the shocks that occurred in May, 1927, on a vertical plane normal to the Gômura fault. (Region III.)

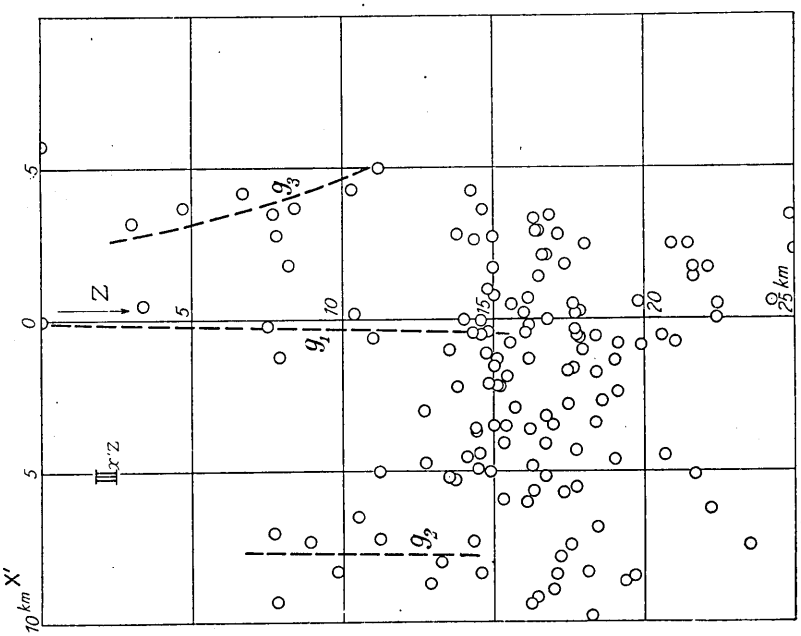

Fig. 32. Seismic foci that lie in region III projected on a vertical plane normal to the Gômura fault. (Foci, $X'>10$ km excluded from this Fig.)

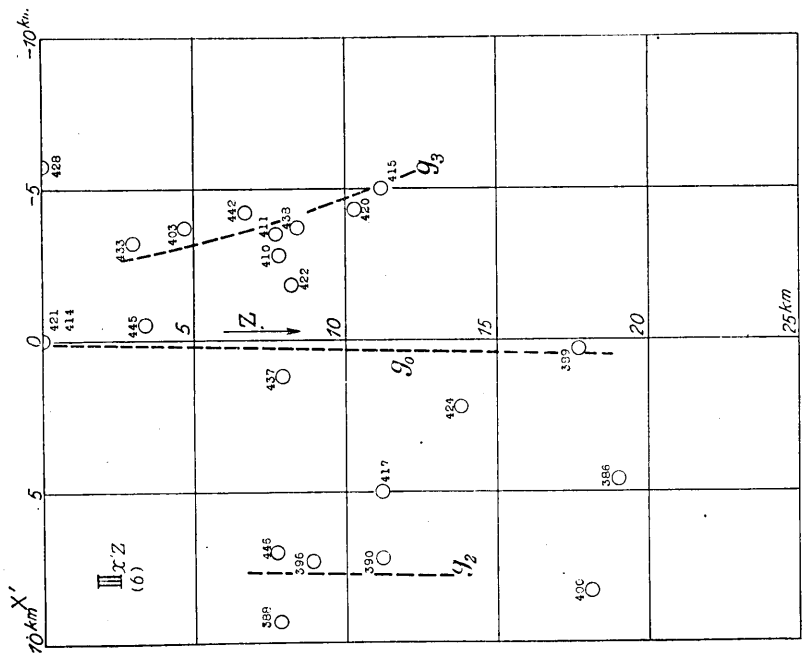

Fig. 31. Distribution of the seismic foci of the shocks that occurred during the period, September 1, 1927~July 15, 1928, in a vertical plane normal to the Gômura fault. (Region III.)

see a remarkable difference in the distribution of the seismic foci, see Fig. 31. The seismically active region had shifted upward, most of the after-shocks having their origins at depths less than 10 km. On the upper prolongation of line g_2 in Fig. 28 are found four foci, while on that of g_0-line three foci. Another conspicuous group of foci is found on the eastern side of g_0-line, where the foci are aligned along the line g_3. Plane g_0 which is nearly vertical extends from the surface of the earth down to a depth of about 15 km. Granting that earthquakes are liable to originate in fault planes, it is then highly probable that plane g_0 is the Gômura fault plane. The plane g_2 is a weak zone running parallel with the Gômura fault.

From the results thus far obtained, the following facts have been revealed:

There exists some bounding surface of a seismically active region that lies nearly horizontally, such as those shown by lines h_0 and h_1. The mean depth of this surface is not stationary, but changes with time.

Other weak zones lying nearly vertical, the position of which could be determined, are those marked g_0 and g_2. The distance between these two planes is about 8 km. Here, we must add that, as shown by calculations, the mean errors in the position of a seismic focus with a depth of about 10 km will not exceed 3 km in horizontal direction. We may therefore say that these are not planes that have appeared as the result of errors in observation.

The distribution of all the foci lying in region III is shown in Fig. 32.

(B) The foci of the shocks in region III will now be projected on a vertical plane parallel to the Gômura fault zone. They were also divided into several classes according to the times of earthquake occurrence, although not in strictly the same way as done previously.

We shall first project the foci of the shocks that occurred during a period of about ten days following the great earthquake, Fig. 33. Let Y' be the distance of epicentre from the X′ axis. The values of Y' are given in Table.

In taking Y' as abscissa and Z the focal depth, as ordinate, the distribution of the foci will be illustrated in a similar manner as we have previously done. It will be seen from Fig. 33 that most of the shocks originated within depths of 15 and 20 km, as already shown in Fig. 26 and Fig. 27. The foci shown by black circles in Fig. 33 are the same as those indicated with the same symbols in Fig. 26. They do not show any regular distribution.

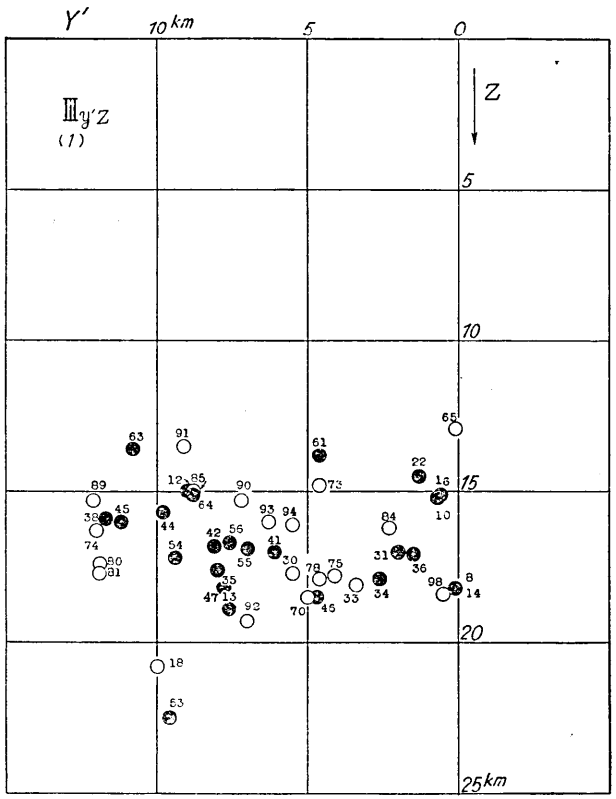

Fig. 33. Distribution of the seismic foci of the shocks that occurred during the period March, 12~17, 1927, on a vertical plane parallel to the Gômura fault. (Region III.)

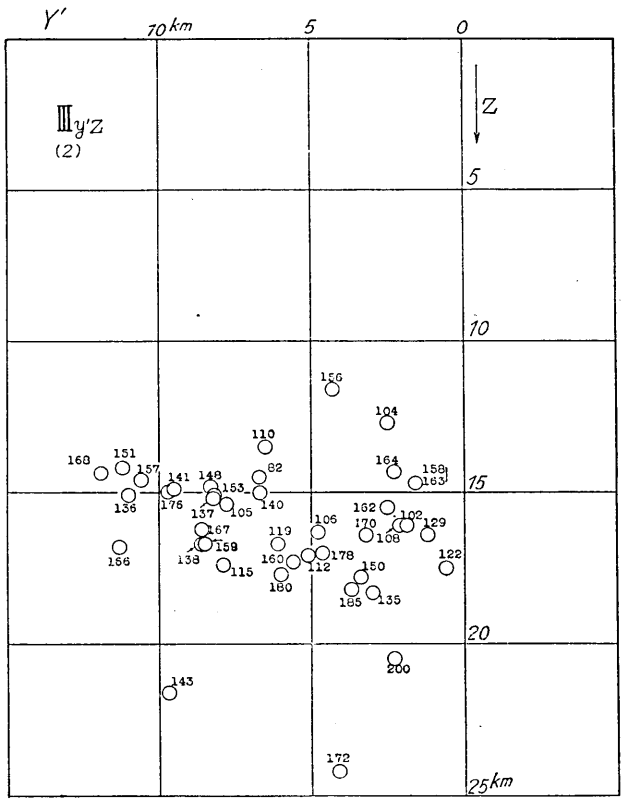

Fig. 34. Distribution of the seismic foci of the shocks that occurred during the period, March 17~April 1, 1927, on a vertical plane parallel to the Gômura fault. (Region III.)

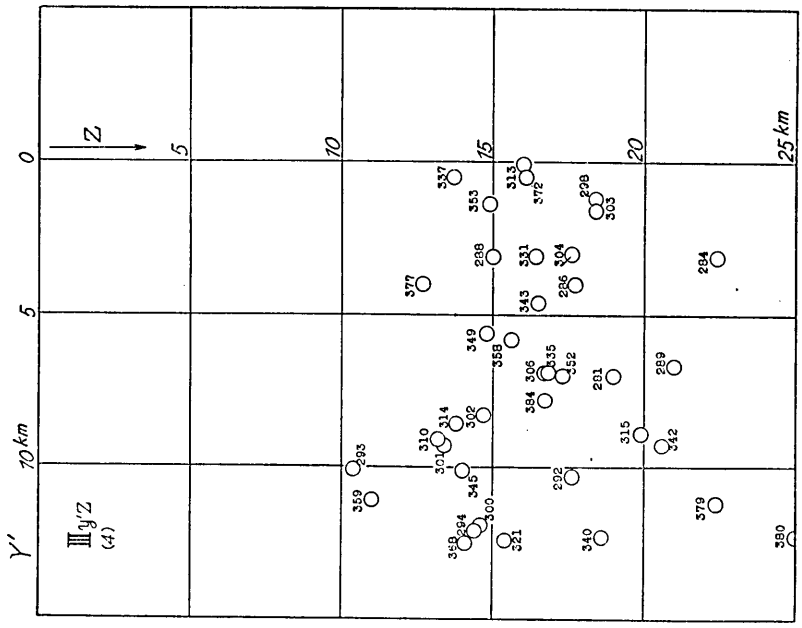

Fig. 36. Distribution of the seismic foci of the shocks that occurred during the period, May 1~August 31, 1927, on a vertical plane parallel to the Gômura fault. (Region III.)

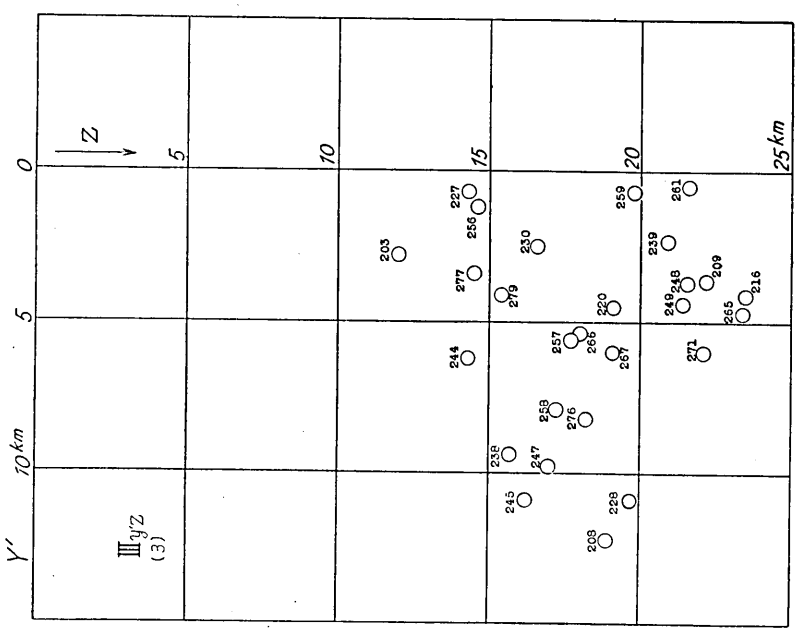

Fig. 35. Distribution of the seismic foci of the shocks that occurred during the period, April 1~30, 1927, on a vertical plane parallel to the Gômura fault. (Region III.)

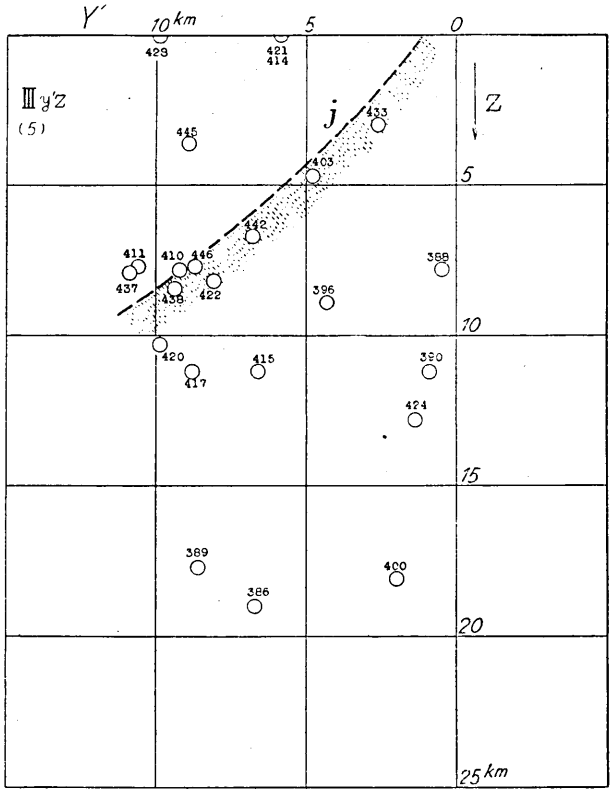

Fig. 37. Distribution of the seismic foci of the shocks that occurred during the period, September 1, 1927~July 15, 1928, on a vertical plane parallel to the Gômura fault. (Region III.)

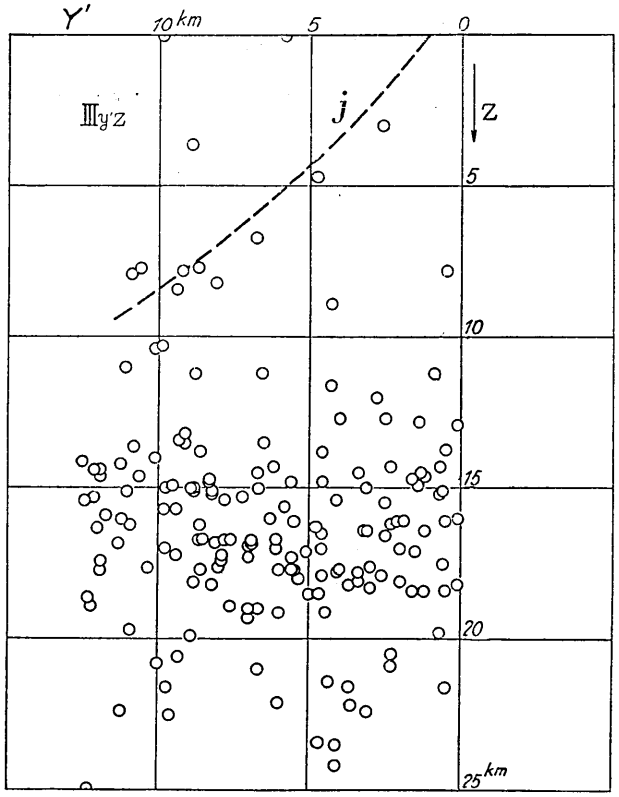

Fig. 38. Seismic foci in region III projected on a vertical plane parallel to the Gômura fault.

The foci of the shocks that occurred during the next period of about two weeks, from March 17～31, were distributed as shown in Fig. 34. A comparison of Fig. 33 and Fig. 34 shows that the seismically active region shifted upward slightly during this period.

In the period that followed, however, the active region changed, the foci being spread over much wider regions than in the case of Fig. 34, see Fig. 35. In the latter figure the distribution of the seismic foci for a period April 1～30 is shown, and in Fig. 36 the distribution of the foci for a period May 1～Aug. 31 is shown.

We shall next project the foci of shocks that occurred during the last period, from Sept. 1, 1927, to the middle of July of the following year. As already pointed out, most of the foci of the shocks were at depths less than 10 km. A conspicuous feature of the seismic foci is that they arranged themselves along a boundary plane, as shown by the hatching in Fig. 37. Excepting foci Nos. 428, 421, 414 and 445, all the foci were distributed in a region lower than this bounding surface. If we extend this surface until it meets the surface of the earth, the surface evidence of this surface will be found to agree fairly well with the Yamada fault line. Granting that the fault zone or the fault plane is the weak zone in which earthquakes are liable to originate, we can say in the same way as we did in the case of the g_0-plane, that this bounding surface is the Yamada fault plane itself.

With respect to the preceding four foci, it should be added that foci Nos. 421 and 414, 445, were situated on plane g_0, while No. 428 was on the earth's surface at a distance of about 6 km east of the Gômura fault zone.

The results here obtained will be very important in connection with the general discussion of seismic foci distribution to be made in the conclusion at the end of this paper. All the foci are projected and shown in Fig. 38.

Block No. II.

We shall now study the foci lying in region II, contiguous northwest of the receding region (see Fig. 24). The eastern boundary of this block, No. II, is the Gômura fault.

(A) Projection on plane $X'Z$.

In projecting the foci of the after-shocks that occurred in March, 1927, on a vertical plane normal to the Gômura fault zone, distance, X' was measured for each focus, their values being given in Table VIII.

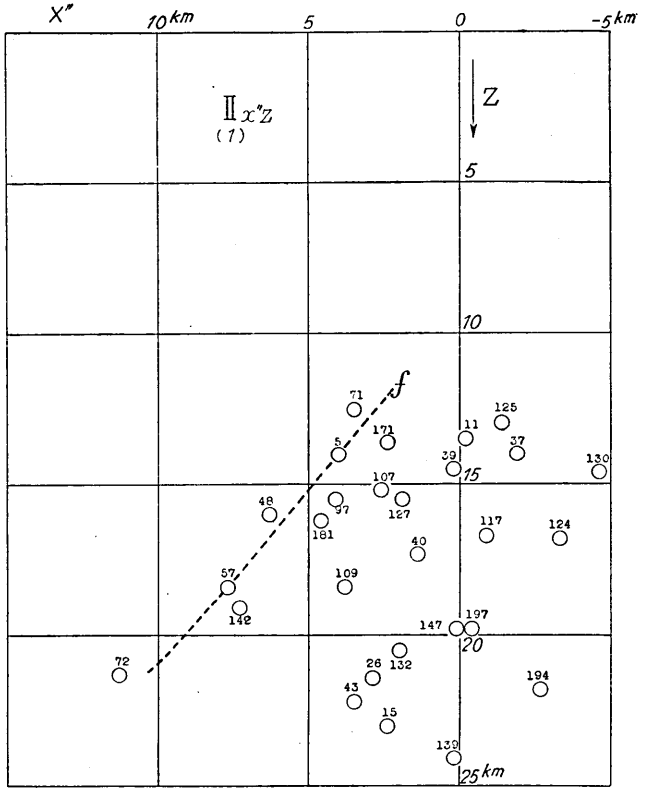

Fig. 39. Distribution of the seismic foci of the shocks that occurred during the period March 12~31, 1927, on a vertical plane normal to the Gômura fault. (Region II.)

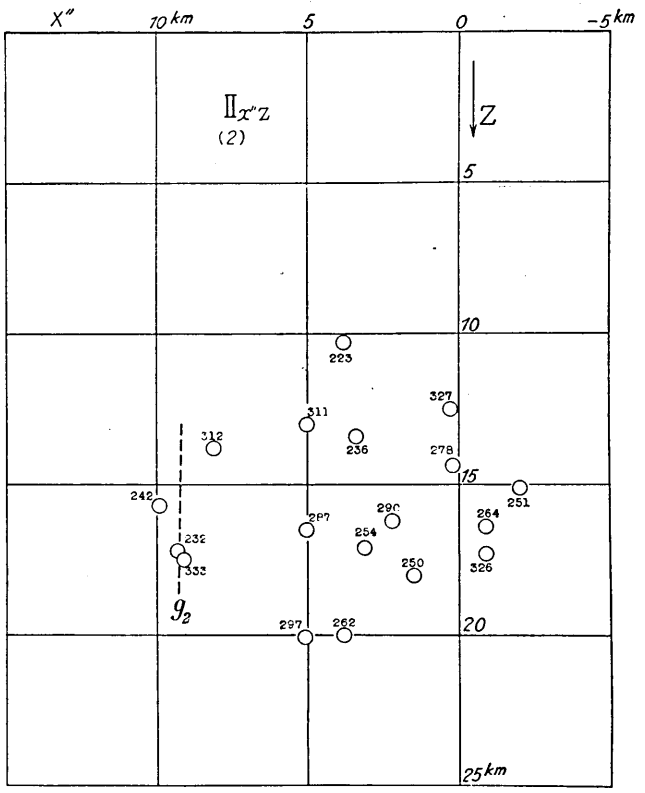

Fig. 40. Distribution of the seismic foci of the shocks that occurred during the period April 1~May 31, 1927, on a vertical plane normal to the Gômura fault. (Region II.)

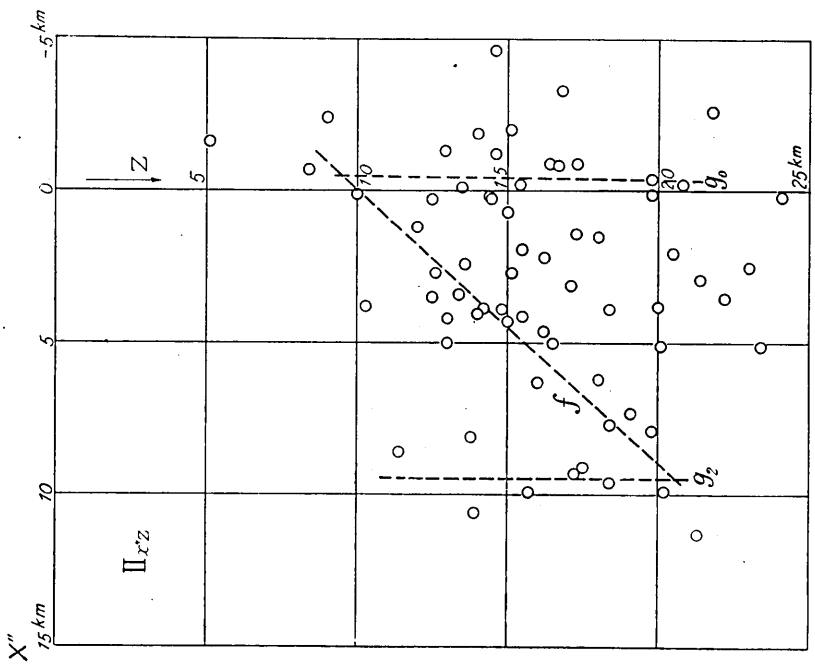

Fig. 42. Seismic foci in region II projected on a vertical plane normal to the Gômura fault.

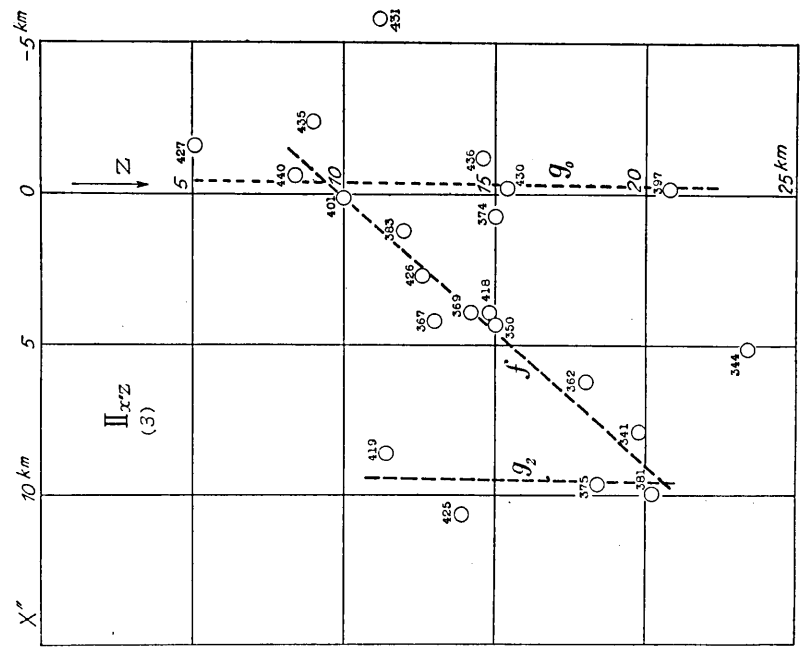

Fig. 41. Distribution of the seismic foci of the shocks that occurred during the period June 1, 1927～July 15, 1928, on a vertical plane normal to the Gômura fault. (Region II.)

By taking X' as abscissa and Z as ordinate we get Fig. 39. The distribution of the foci do not call for any special comment, although it suggests the existence of a boundary surface to the seismically active region as indicated by line f. The existence of this surface will be confirmed by projecting the foci of the shocks of later occurrence.

Most of the shocks that occurred in the next period, April 1～May 31, had their origins at places deeper than 13 km. Of these foci, four, viz., Nos. 312, 242, 232, 333, could be seen to be grouped about line g_2. From the way these foci arrange themselves, we may suspect the presence of certain weak zone or fault plane, see Fig. 40.

For the next period, June 1, 1927～July, 1928, the seismic foci showed a distribution as shown in Fig. 41. In this figure, the existence of the weak zones indicated by g_0 and g_2 can be easily confirmed. Another weak zone, indicated by f in the same figure will be the same surface indicated by the same symbol in Fig. 39. The plane f intersects with planes g_0 and g_2 at an angle of about 45°. Plane g_0 here determined will be the northern extension of plane g_0 in region III. This is probably the Gômura fault plane. Plane g_2 may also be the northern extension of plane g_2 in region III. The distance between these planes which are about 9 km, becomes somewhat greater than that determined for region III, although owing to errors of observation, we are not certain of the details. By projecting all the foci in the above three figures we obtain Fig. 42.

(B) Projection on plane $Y'Z$.

The foci in the same region will now be projected on a vertical plane parallel to the Gômura fault zone. In this projection Y' is measured from the new axis X'', which is parallel to the X' axis. The new origin of coordinates is taken at point 0_2 (Fig. 24). The values of Y' of the foci lying in this region are given in Table VIII.

The foci of the shocks that occurred during the first period, the same as shown in Fig. 39, were projected on the vertical plane just mentioned, with the result as shown in Fig. 43. No regular distribution of foci can be seen in this diagram.

In Fig. 44, the distribution of the foci of the shocks that occurred during the second period is shown. It will be seen from Figs. 43 and 44 that a certain boundary of the seismically active region exists as shown by line j. The boundary here determined is the lower extension of line j, already shown in Fig. 38. Another seismically weak zone was determined as indicated by line k.

Except two foci, Nos. 427 and 440, the foci of the shocks that occurred during the last period may be seen grouped about two lines, j

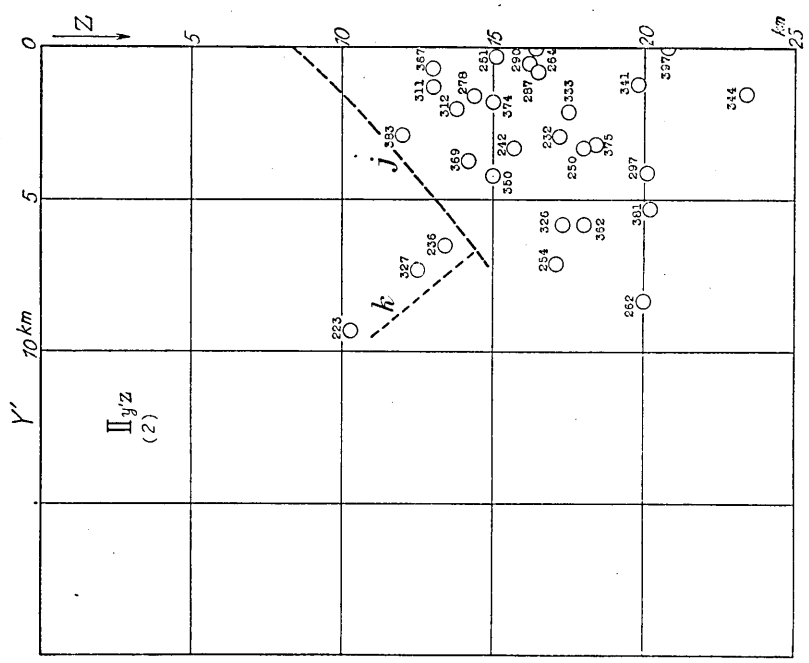

Fig. 44. Distribution of the seismic foci of the shocks that occurred during the period April 1～Oct. 31, 1927, on a vertical plane parallel to the Gômura fault. (Region II.)

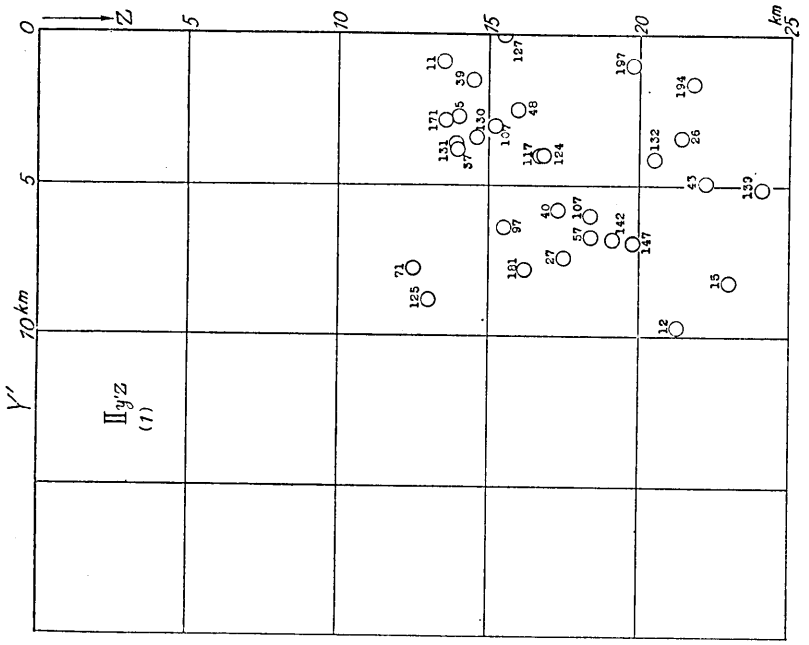

Fig. 43. Distribution of the seismic foci of the that shocks occurred during the period March 12～31, 1927, on a vertical plane parallel to the Gômura fault. (Region II.)

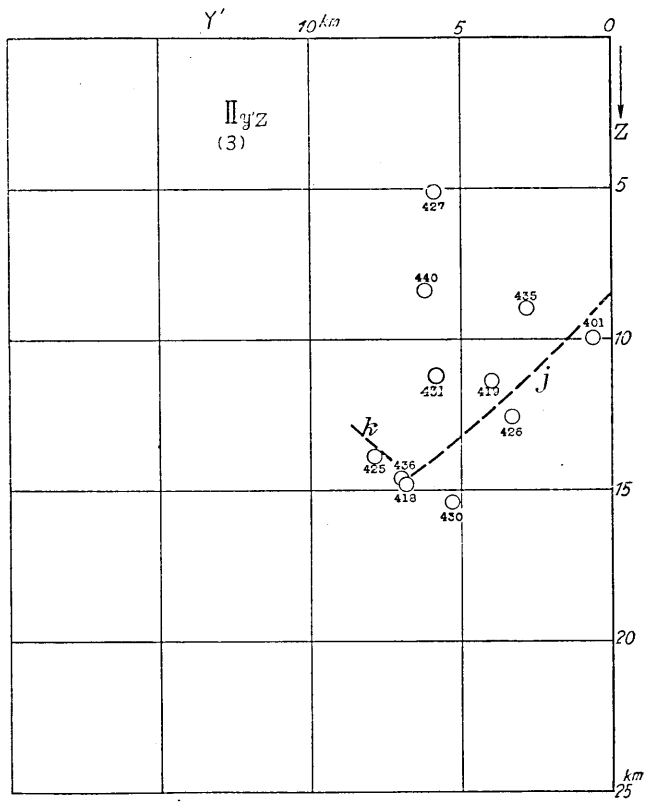

Fig. 45. Distribution of the seismic foci of the shocks that occurred during the period November 1, 1927~July 15, 1928, on a vertical plane parallel to the Gômura fault. (Region II.)

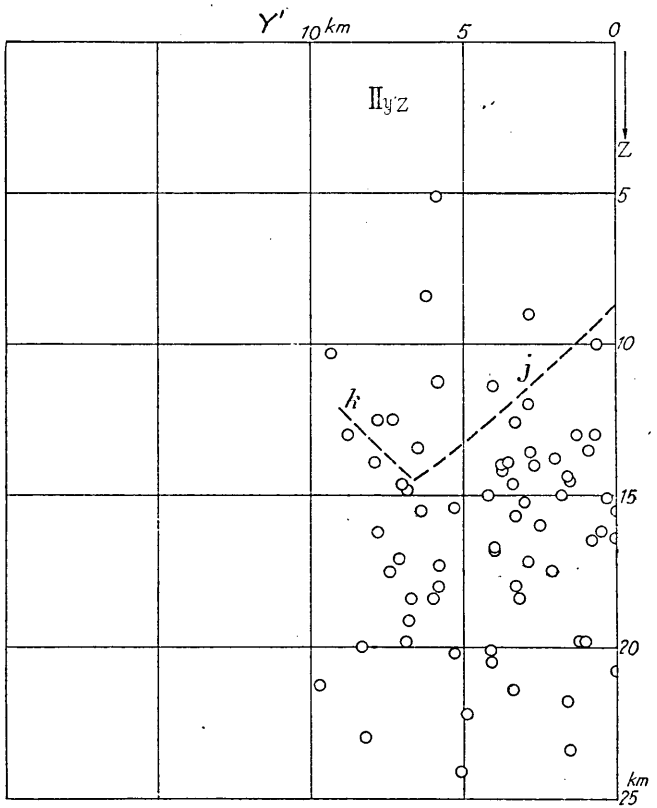

Fig. 46. Seismic foci of the shocks that occurred in region II projected on a vertical plane parallel to the Gômura fault.

and k. These two foci are of shocks that originated in the weak zone g_0, probably in the Gômura fault plane (see Fig. 45).

By projecting all the foci in the region now in question, we can see that the seismically active region was bounded by plane j (perhaps by the Yamada fault plane) in the south, and by plane k in the north. These two planes intersect nearly at right angles at a depth of 15 km. The results here obtained is also important in connection with the general discussion of the distribution of seismic foci of the Tango after-shocks to be made later.

Block No. I.

Judging from the distribution of the epicentres of the Tango after-shocks, regions lying on the Japan Sea were also active after the great earthquake, although the shocks were less in number than in other regions, such as No. II and No. III.

Here the studies were limited to seismic foci that had their epicentres in region I in Fig. 24. The eastern boundary of land block No. I was assumed to be the northern extension of the Gômura fault zone. This assumed boundary is not the extension of the Y′ axis, which shows the mean trend of the Gômura fault zone as found on the actual land surface. It makes an angle of about 10° with the Y′ axis. This new axis was taken such that, in the north it passes near the epicentres of the after-shocks deduced as having occurred virtually on the earth's surface, and in the south meets with the northern extremity of the Gômura fault. The foci of the shocks just referred to that originated on the earth's surface may be seen to be grouped in a comparatively narrow area, the centre of which lies at a distance of about 15 km from the coast line. Needless to say, the foci in the contiguous blocks were also taken in consideration in our studies. We shall first project the foci in region I on a vertical plane normal to the Y″ axis.

(A) Projection on plane $X'''Z$.

As the foci were not sufficiently numerous to divide into classes according to the times of earthquake occurrence, we shall, in this projection, take all the foci that lie in this region and show their distribution in one diagram, Fig. 47. The values of X' are given in Table.

In Fig. 44, we see that the foci were grouped on lines g_0 and g_1. Four foci of the shocks that had their deduced origins on the earth's surface may be seen to be grouped about the former line, on two sides of which line several foci are distributed from the earth's surface to depths greater than 10 km. The plane g_0 in Fig. 47 may be the

northern extension of the Gômura fault plane.

Another weak zone is indicated by line g_1 in the same diagram, on both sides of which line several foci may be seen to be grouped. The existence of this weak zone has already been commented on in connection with region III, in which latter region its existence was less certain than in region I.

Another weak zone from which after-shocks originated is that indicated by line g_2. This zone is probably the northern extension of the weak zone, g_2, which was already found in region II and III. But in view of the small number of foci its actual existence is uncertain.

(B) Projection on plane $Y''Z$.

The foci in region I will now be projected on a vertical plane parallel to the Y'' axis. The values of Y'' are given in Table IX.

The results are shown in Fig. 48. A noteworthy fact is that the foci, with only a few exceptions, are in a region lying north of (left in diagram) and below the curve indicated by l. The boundary dips south. Assuming certain errors in the position of the seismic foci we make some corrections in the position of the foci that lies on curve l, when the boundary can then be indicated somewhat schematically by a new curve l'. There are only four foci lying on the upper, or southern side (right-hand side Fig. 48), namely, Nos. 423, 269 and 376, 443. Of these foci Nos. 423 and 376 are situated on line g_0, see Fig. 47, while No. 269 was on the earth's surface, east of line g_0, see also Fig. 47. Only one focus, No. 443, lies west of plane g_0 and on the upper side of curve l. It would lie on line g_1 if it were projected on a vertical plane normal to the Y'' axis, see Fig. 47. On the other hand, the focus just mentioned seems to lie on the upper prolongation of line k which was already shown in Fig. 46; the details will be given later.

The results so far obtained are also important in connection with the general discussion to follow on the distribution of the seismic foci.

Block No. IV.

In our previous paper,[13] four land blocks were taken on the south-eastern side of the Yamada fault line, and the distributions of the seismic foci lying in these blocks were shown in different diagrams. The projection of the foci, however, on a vertical plane normal to the faults trending from NE to SW (faults a, b and c in Fig. 24) showed similar results for the foci lying in each block. In the present study, therefore, a wider region, for projection as indicated by IV in Fig. 24

13) N. NASU, *loc. cit.*

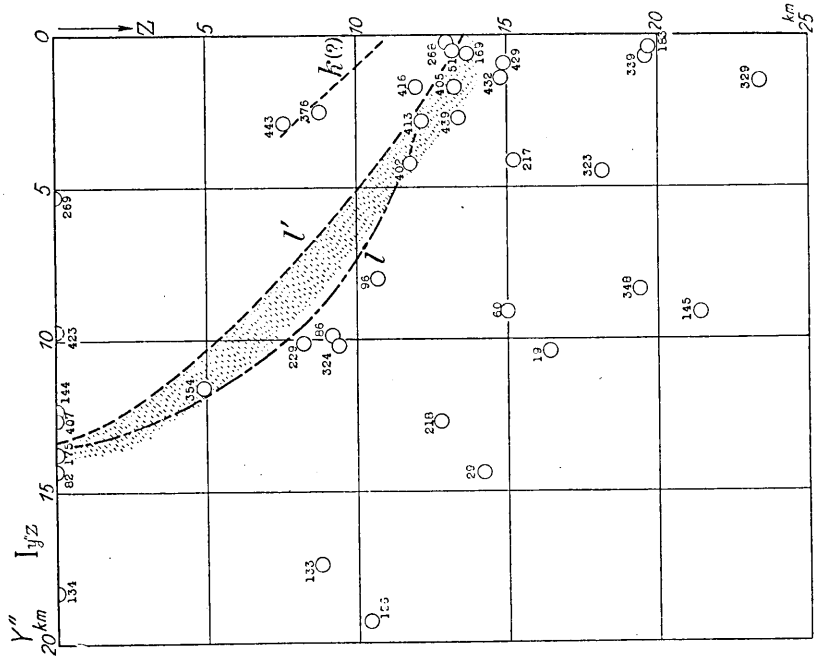

Fig. 48. Distribution of the seismic foci lying in region I projected on a vertical plane parallel to the Y'' axis in Fig. 24.

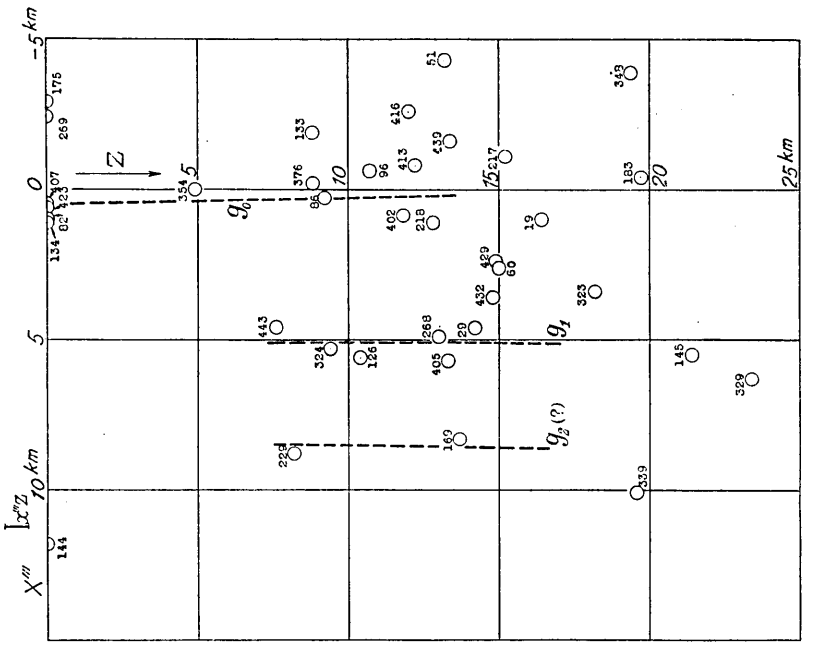

Fig. 47. Distribution of the seismic foci lying in region I on a vertical plane normal to the Y'' axis in Fig. 24.

was taken and the foci in this region were projected on two vertical planes differing from those that were taken in the case of regions II and III. Coincidentally, the major geomorphologic faults in this region run parallel to each other and also nearly parallel to axis Y in Fig. 24, that is, nearly perpendicular to the line joining Maiduru and Kinosaki. For this region, the two planes of projection were taken such that one shall be parallel to the X axis and the other to the Y axis.

In this region the after-shocks were particularly active after the strong earthquake of April 1, 1927. This strong earthquake occurred in the region now under consideration. The seismic foci of this earthquake is No. 201. It was followed by numerous minor shocks, the daily number of these after-shocks suddenly increasing during the first few days of April. For this reason the number of foci in this region was considerable, so that they were divided into three classes according to the times in which the earthquakes occurred.

(A) Projection on plane XZ.

We shall take the plane of projection parallel to the X axis and project all the foci on this plane. The values of X of the foci lying in this region are given in Table X.

The foci of the shocks that occurred before the strong earthquake of April 1 was distributed as shown in Fig. 49. Most of the shocks occurred on the deeper side of plane indicated by curve m. The focal depths of these after-shocks are mostly less than 20 km. and near point, $X=19$, $Z=17$ km, the seismic foci here will be seen to be grouped very thickly.

The foci of the shocks that followed the strong earthquake of April 1 will be seen to be grouped in a region lying somewhat more on the eastern side (on the right-hand side in the diagram) than those in the foregoing diagram, see Fig. 50. The seismic activity undoubtedly migrated eastward. In Fig. 50, the foci are densely grouped in a region bordered by four lines, $Z=10$, $X=15$, $Z=14$, $Z=19$ km, the region in which the foci are very few in the previous diagram (Fig. 49). The foci in Fig. 50, however do not lie in the region lying on the upper side of curve m, that is, they have the same distribution as that already shown in Fig. 49, with one exception No. 305.

The foci of the shocks that occurred during the last period were distributed at depths less than 17 km, Fig. 51. Of these, three foci were situated at depths less than 10 km. There is little doubt that seismic activity migrated upward during this period. Three shocks occurred at depths less than 10 km, that is, in a region lying on the

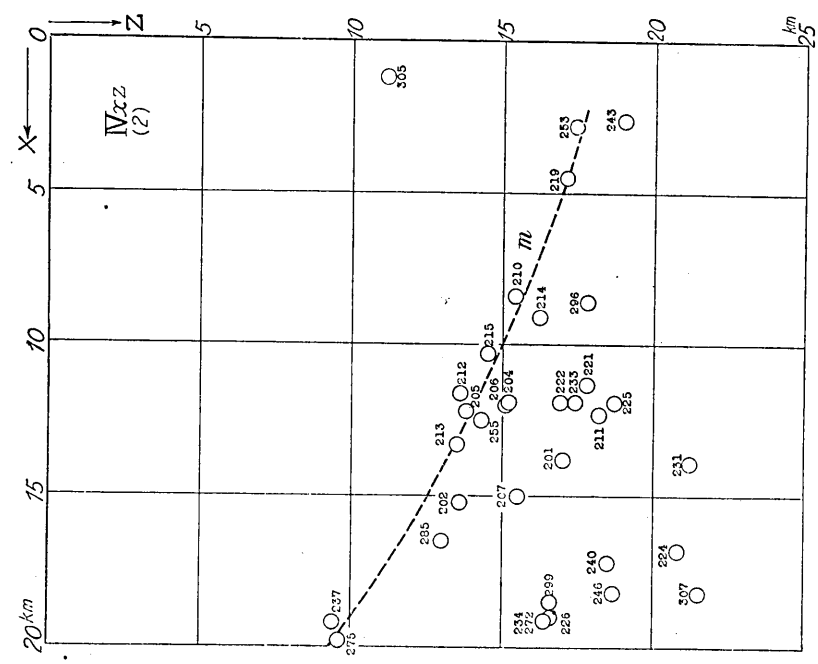

Fig. 50. Distribution of the seismic foci of the shocks that occurred during the period, April 1~May 9, 1927, on a vertical plane normal to the Y axis in Fig. 24. (Region IV.)

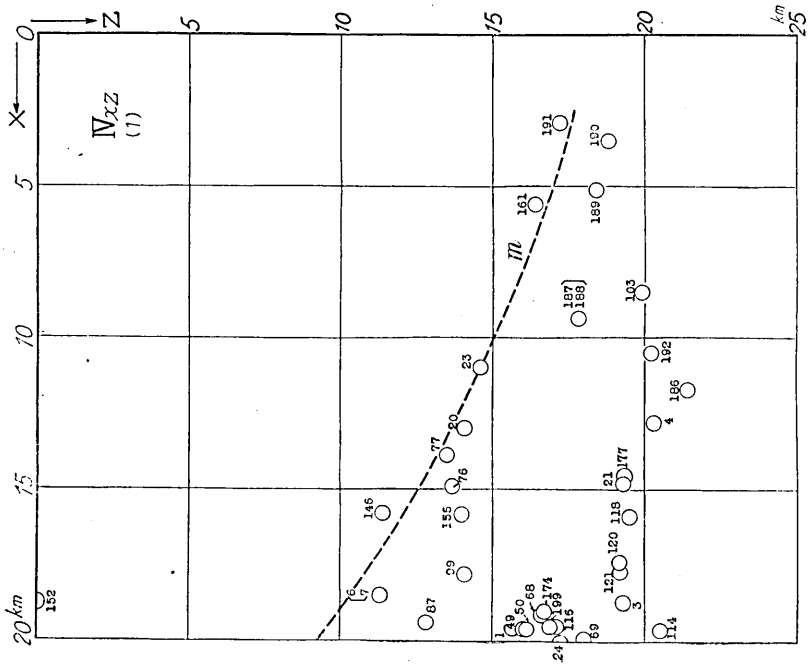

Fig. 49. Distribution of the seismic foci of the shocks that occurred during the period, March 12~31, 1927, on a vertical plane normal to the Y axis in Fig. 24. (Region IV.)

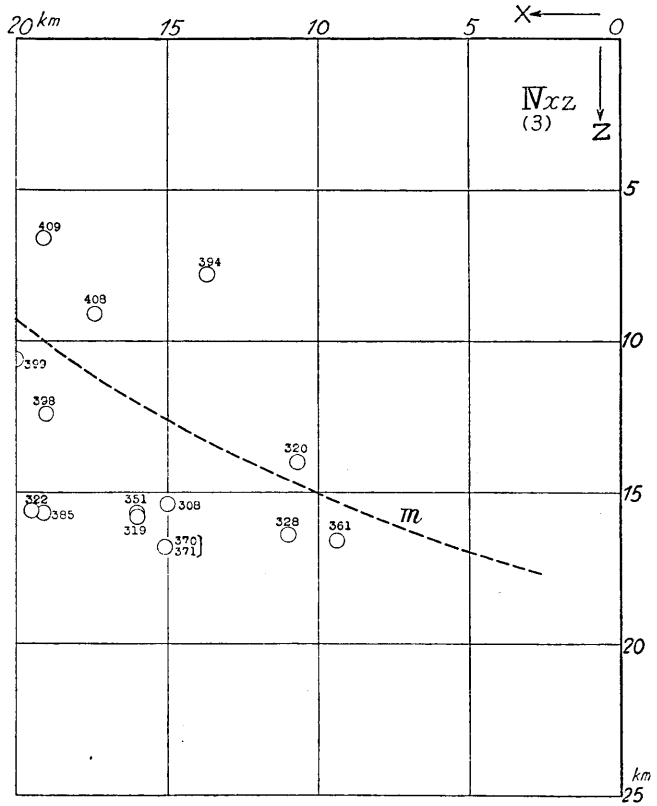

Fig. 51. Distribution of the seismic foci of the shocks that occurred during the period, May 9, 1927~July 15, 1928, on a vertical plane normal to the Y axis in Fig. 24. (Region IV.)

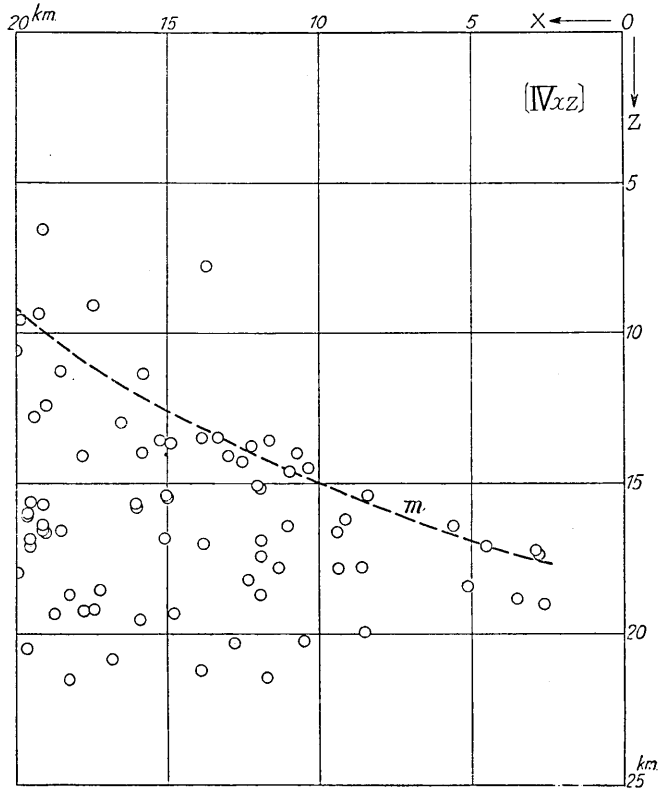

Fig. 52. Seismic foci lying in region IV projected on a vertical plane normal to the Y axis in Fig. 24.

upper side of the boundary which was already shown by curve m in the foregoing figures. The existence of the boundary of the seismically active region cannot be known from the distribution of the seismic foci shown in Fig. 51 alone. The distribution of all the foci in the foregoing three diagrams is shown in Fig. 52.

(B) Projection on plane YZ.

In this projection, the foci were divided into three classes according to the times of earthquake occurrence, although the classification is not the same as before. The values of Y are shown in Table X.

The distribution of the foci of the shocks that occurred before the strong earthquake of April 1 (No. 201) is shown in Fig, 53. In this diagram, no regular distribution of the foci can be seen, except that there exists a certain boundary of the seismically active region at a depth of about 15 km. The boundary is nearly vertical, as indicated by line p. The existence of this boundary will become evident by projecting the foci of the shocks that occurred during the next period.

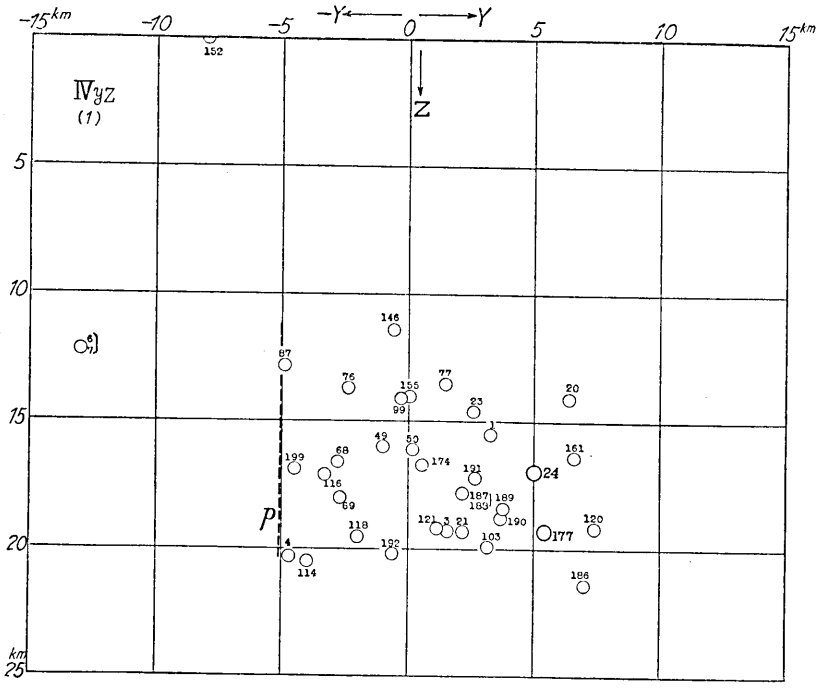

Fig. 53. Distribution of the seismic foci of the shocks that occurred during the period, March 12~31, 1927, on a vertical plane normal to the X axis in Fig. 24. (Region IV.)

The foci of the shocks that occurred during the next period, April 1～May 30, may be grouped on both sides of two lines p and q_1, Fig. 54. Line p indicates the southern boundary of the seismically active region just mentioned. Line q_1 indicates another weak zone dip-

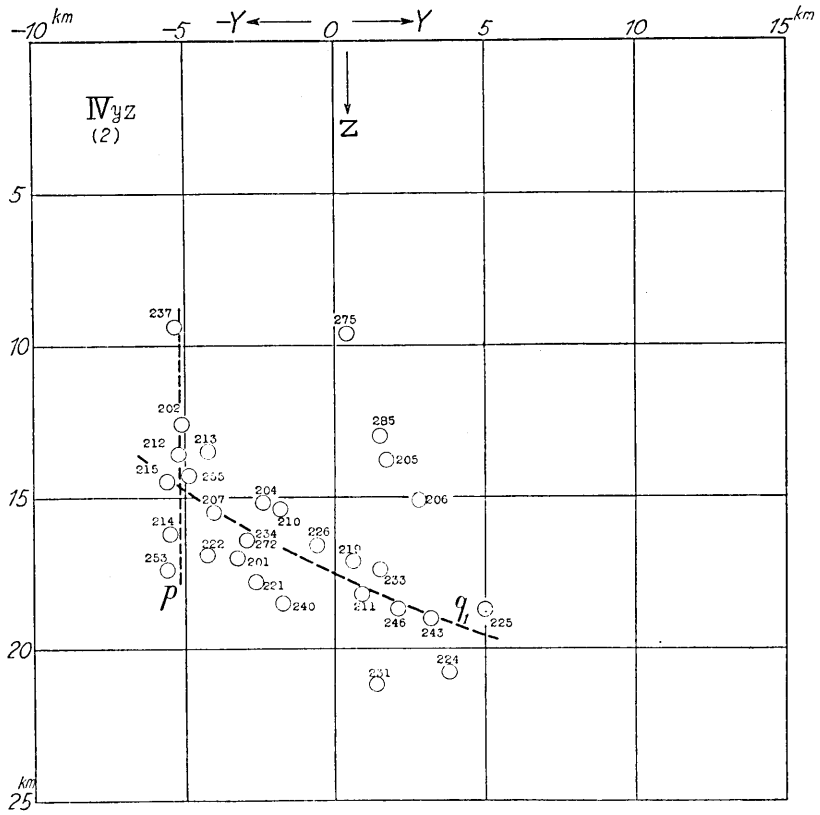

Fig. 54. Distribution of the seismic foci of the shocks that occurred during the period, April 1～May 1, 1927, on a vertical plane normal to the X axis in Fig. 24. (Region IV.)

ping north. It may be said that most of the foci of the shocks that occurred during a month following the strong earthquake of April 1 show fairly regular distribution. It should be added that this strong earthquake originated near the intersection of the two planes indicated by lines p and q_1.

The foci of the shocks that occurred during the last period, from

June, 1927, to the middle of July, 1928, show a distribution as shown in Fig. 55. The distribution of the foci makes it clear that the seismic activity migrated upward during this period. Although most of the foci may be seen to be grouped about line q_2, which is nearly parallel to line q_1, in Fig. 54, the former line lies in a shallower region than the latter. The boundary, p, may also be seen in this diagram. The foci Nos. 409, 408, 394, 378 are of shocks that originated in other weak zones, but the details are unknown. The distribution of all the foci that lie in this region is shown in Fig. 56.

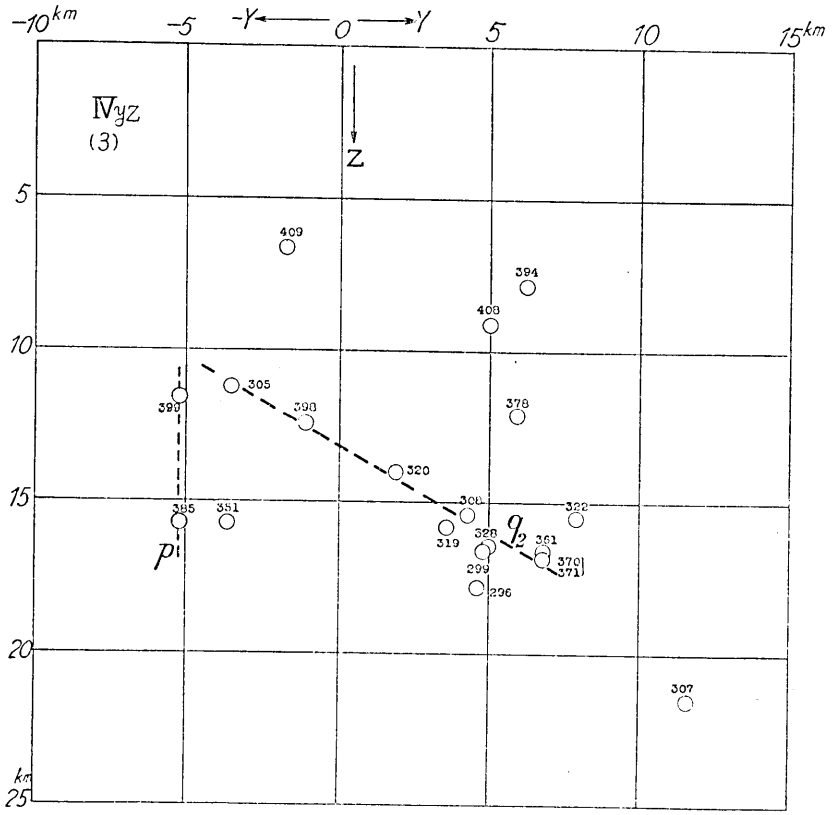

Fig. 55. Distribution of the seismic foci of the shocks that occurred during the period, May 1, 1927~July 15, 1928, on a vertical plane normal to the X axis in Fig. 24.

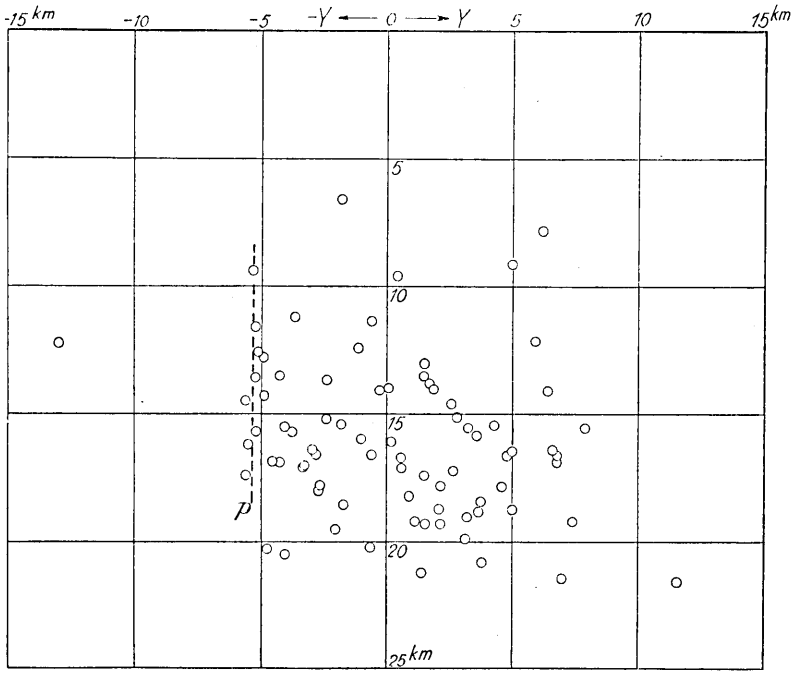

Fig. 56. Seismic foci lying in region IV projected on a vertical plane normal to the X axis in Fig. 24.

Conclusions on the Stereometrical Distribution of the Tango After-shocks.

In has been made clear by the stereometrical distribution of the seismic foci referred to, that most of the Tango after-shocks that originated west of the Gômura fault zone could be seen to be grouped about planes running parallel to the fault zone that appeared on the earth's surface at the time of the great earthquake. The planes which are determined from the distribution of the seismic foci are undoubtedly the weak zones that actually exist in the earth's crust where earthquake are apt to originate. By projecting the foci lying west of the Gômura fault on a vertical plane normal to the same fault, it was found that some of the weak zones are nearly vertical planes, running parallel with the Gômura fault, as well as with some other weak zones lying nearly horizontally. The arrangement of these weak zones can clearly be seen particularly in regions II and III. One of these vertical planes ought to be that whose surface trace was that of the Gômura fault zone as observed on the ground. This plane is indicat-

ed in the foregoing studies by line g_0. Judging from the distribution of the seismic foci on this line it is possible to say that along this weak zone the earthquakes originated from the earth's surface to a depth greater than 10 km, and further that this zone runs through the earth's crust that forms the land as well as through the earth's crust that lies under the Japan Sea.

Another conspicuous weak zone, which is also vertical and parallel to the Gômura fault zone, is that indicated by line g_2. In this weak zone, earthquakes originated at fairly shallow depths (less than 10 km) during the later half of the period of our observations, although they did not occur on the earth's surface. This plane may be the western boundary surface of the land blocks bordered by the Gômura fault in the east. The distance between this plane and the Gômura fault plane is 8～9 km, which is the probable distance of the boundaries of the land blocks that were determined by precise levellings carried out in various parts of Japan.

The other weak zone running athwart the vertical zones just mentioned is that found very clearly in region II, and indicated by line f. This weak zone intersects the vertical ones at an angle of about 45°. The existence of this weak zone is not surprising in the light of experiments that have been made in connection with the formation of cracks in isotropic homogeneous materials as briefly referred to in an earlier part of this paper.

By projecting the foci that lie west of the Gômura fault zone on a vertical plane parallel to the fault zone, we find that the shocks originated outside the region that is bounded by the earth's surface and the planes indicated by lines j and l. On line j, the foci of the shocks were distributed within depths of 3 km and 15 km. The plane indicated by this line is probably the Yamada fault plane. It may be said from the distribution of the seismic foci that the Yamada fault is not a mere surface phenomenon, such as the flexure that appeared at the time of the great earthquake, but extends downwards to a considerable depth–in this case as much as 15 km. The surface trace of the other plane, l, is vague, owing to the reason that it lies on the sea bottom where no perceptible changes can be seen in the chart on either side of this imaginary surface trace.

Although in the region southeast of the Yamada fault line, the seismic foci did not show any remarkable features connected with their distribution, yet by projecting the foci in this region on a vertical plane normal to the major geomorphologic faults lying there (faults a, b, c in Fig. 24) it was found that the origins of the shocks were

mainly confined to a region lying below curve m. It is possible that there exists certain boundary surface of the seismically active region which could be indicated by curve m.

By projecting the foci in the same region on a vertical plane parallel to the major faults just mentioned, the southern boundary of the seismically active region can fairly accurately be determined. This boundary is indicated by line p. Further, in taking only the foci of the shocks that occurred during the two months following the strong earthquake of April 1, we can obtain a fairly regular distribution of the seismic foci such that the foci may be seen to be grouped about two lines, p and q_1.

We shall next attempt a brief explanation of the migration of seismic activity along certain weak zones. In our study, the earthquake foci were divided into several classes according to the times of earthquake occurrence, and the distributions of the foci shown for each of these classes. The results obtained show that seismic foci belonging in a certain class may group themselves about certain lines. According to the class of foci projected, the lines assume different positions. For example, in region III, the foci of the shocks that occurred during the 8 days that followed the great earthquake could be seen to be grouped about lines g_0 and h_0, while, the foci of the shocks that occurred in the next period could be seen to be grouped about lines g_0 and h_1. As will be seen from Figs. 26, 27, 29, line h_4 lies in a region somewhat shallower than line h_0 — a fact suggesting that the seismically active region migrated upward. The upper boundaries of the active region indicated by these lines are nearly parallel to each other and lie nearly horizontally. The same may be found in the case of lines q_1 and q_2 which were determined from the distribution of the seismic foci lying in region IV. Another noteworthy fact is that, in region II, the shocks that occurred during the later half of our observations had their origins in shallow places and their foci may be seen to be grouped about lines j and k, while in region III the shocks were particularly active in shallow places and their foci aligned themselves along lines g_3. From the facts so far referred to, it is undeniable that the seismic activity migrated upward during the later half of our observations.

It must be added that the horizontal boundaries of the seismically active region just mentioned change their position upward with time, so that in order to determine this horizontal boundray it is best first to divide the foci into several classes according to the times of earthquake occurrence, and then project each class of foci in a separate

diagrams by itself. To project all the foci, regardless of the times of earthquake occurrence, would sometimes end in failure to obtain desired results.

Extended studies of the stereometrical distribution of the seismic foci of the Tango after-shocks enable us to visualise the form and the movement of the land block that played such an important part in the great Tango earthquake. In the following paragraphs an attempt will be made to describe the results of investigation thus obtained.

By projecting on the vertical plane that passes through the surface traces of the Gômura fault, all the seismic foci of after-shocks that occurred within a distance of about 10 km to the west of this fault zone, it was found that in the triangle enclosed by the three lines corresponding to, (1) the projection of the earth's surface, (2) the plane that is probably that of the Yamada fault, and (3) the plane designated l or l', no after-shocks at all, except one, wereexper ienced there since the beginning of the observations that were begun immediately after the great earthquake, up to the end of July, 1928, the following year. We may state with confidence, then, that the triangle corresponds to the cross-section of certain blocks that lie on the western side of the Gômura fault zone, where they are cut by a vertical plane parallel to the fault itself.

Strictly speaking, the lower part of the same block has somewhat complicated form. The block now in question is bounded in the north not only by plane l, but also by plane k. The latter plane was deduced from the distribution of the seismic foci lying in region II. If we take plane k in consideration and visualise the cross-section of the block, then the results become as shown in Fig. 57.

In the lower part of the block just mentioned where planes j, k and l meet, several foci of shocks that occurred in the later half of our period of observations are fairly densely distributed. Most of the foci of these shocks may be seen to be grouped about lines j, k, l. From this it may be said that the seismic activity migrated in both directions, one upward along plane j and the other along planes k and l, although the activity mostly migrated along the first plane, that is the Yamada fault.

It should be added that the foci lying inside the region corresponding to the cross-section of the foregoing land block when projected on a vertical plane parallel to the Gômura fault zone are of shocks that originated in the Gômura fault plane, or of the shocks that originated in the contiguous block lying east of the fault plane just mentioned. The solitary focus that lies in the triangle, the cross-section just

referred to, is No. 443, that of the shock that occurred on June 20, 1928. It lies on line g_1 when projected on a vertical plane normal to the Gômura fault line (Fig. 47). The upper part of the weak zone indicated by line g_1, which might extend upward and inside the land block just mentioned, suggests that some changes in the form of the land block took place in its lower part about 15 months afterward the great earthquake.

On taking the plane of projection normal to the Gômura fault, it will readily be noticed that land mass lying outside of the land block, the vertical section of which was deduced in the foregoing, may be cut up into several small blocks by planes parallel to the Gômura fault plane. In the land mass lying north of the block just mentioned and in the Japan Sea, are three planes which are indicated by projections marked g_0, g_1, g_2, see Fig. 47; and in that lying on the southern side of plane j, the Yamada fault plane, by the same notations are also indicated three planes. But, the existence of plane g_2 is not certain in the former land mass, as also g_1 in the latter land mass. Though the arrangement of the seismically weak zones differs somewhat, there is no question that these weak zones are the boundary of the land blocks that are nearly parallel to the Gômura fault plane.

We shall now visualize the form and the movement of the land block that played such an important part in the recent great earthquake: that is, the block west of the Gômura fault.

Firstly, the block has the form of a triangular prism with one of its side on the earth's surface and its base on, or parallel to the Gômura fault plane.

Secondly, the mechanism as a result of which the present destructive earthquake occurred may be visualised somewhat as follows: Initially, the equilibrium that had obtained in the Tango block was disturbed along the old fault plane, resulting in the new Gômura fault, causing the land block on the western side of this fault to be detached from the surrounding body along the weak zones represented by the Yamada fault plane and the plane marked l. The wedge-shaped block thus formed was then elevated and shifted towards the south. The formative process of this block may be regarded in the light of a very ordinary and natural process, akin to that in which a thick wall-like material is cracked by a shearing force, although in our case the force might act nearly parallel to the walls.

As to how much the block was bodily displaced we have no means of knowing, since the block is not a perfect rigid body, although its mean bodily displacement can be deduced from the results of the pre-

and post-earthquake triangulations carried out in the seismic district. Prof. Imamura and F. Kishinouye[14] recalculated the displacements of the geodetic points, the primary and secondary points, lying on the surface of the land block just referred to, reducing each displacement parallel to the Gômura fault zone. The results showed that the triangulation-marks lying on the eastern side of the Gômura fault were displaced towards the north, while those of the western side of the same fault had shifted towards the south, and that the amounts of these displacements diminished with increasing distance from the fault zone. The displacements at Simooka, Isanagosan, and Nyôo, deduced from the observations of 1884～1888 and August 1927, are shown in the table that follows. These triangulation-marks lie on the surface of the wedge-shaped block in question.

(x), (y)	Simooka	Isanagosan	Nyôɔ
Distance from the fault (x)	−0·7 km	−4·7 km	−7·0 km
Displacement parallel to the fault (y)	−127 cm	−48 cm	−87 cm

where −x=towards W; −y=towards S.

It the deformation of the land block be admitted as having been caused by its movement, then the mean displacement of this block can be calculated by taking the mean value of y from the foregoing table. The mean displacement thus obtained is −87 cm, that is, 87 cm towards S., or exactly towards SSE.

It is of no less interest to study the vertical movement at the time of the great earthquake of the land block under consideration. From the results of precise levellings, changes in the heights of the land surface are known to be as shown in Fig. 58. This Fig. is taken from the report of the levellings that were carried out by the Military Land Survey.[15] In the map in Fig. 58 the regions that rose up at the time of the great earthquake are shown with hatching, contours for every 20 cm

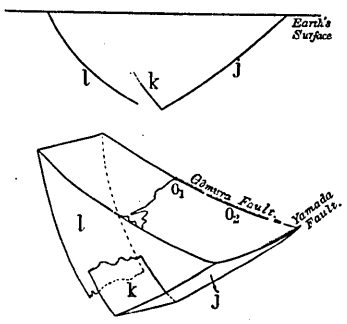

Fig. 57. The wedge-shaped land block that are deduced from the stereometrical distribution of the seismic foci of the Tango after-shocks. (Upper = cross-section, Lower = side view of the land block.)

14) A. IMAMURA and F. KISHINOUYE, "On the Horizontal Shift of Dislocation accompanied by the Recent Destructive Earthquakes in the Kwantô District and in Tango Province," *Bull. Earthq. Res. Inst.*, **5** (1928), 35.

15) *Report of the Military Land Survey*, (November 1930).

upward displacement being drawn with full-lines and those for every

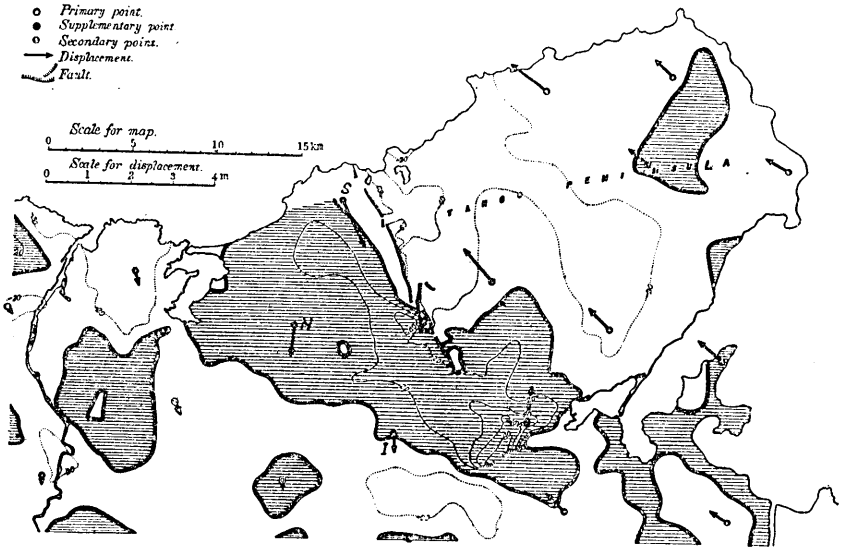

Fig. 58. Map showing the displacements of the triangulation-marks and the changes in level in the Tango district.
(S=Simooka, N=Nyôo, I=Isanagosan.)

20 cm downward displacement in dotted lines. In Fig. 58 we see that the Tango peninsula which was displaced as a whole towards the northwest showed a general subsidence of about 20 cm. Most of this subsidence took place at the time of the great earthquake. The region east of the Gômura fault zone, and adjacent to it, showed a remarkable subsidence of more than 70 cm. Near the northeastern extremity of the Peninsula are three small upheaved areas, the extents of upheaval in them being less than 7 cm.

As to the vertical changes in the surface of the wedge-shaped block now under consideration, we may say that most parts of its surface showed upheaval. We see in Fig. 58, that a fairly large elevated area lies west of the Gômura fault adjacent to it. The width of this area (here by width is meant distance from the fault just mentioned) gradually lessens in the southern part. The extent of upheaval showed increase with decreasing distance from the Gômura fault zone. The region that is enclosed within the full-line contour, indicating a 20 cm upheaval, lies lengthwise, parallel with the Gômura fault. In the region lying north of the Yamada fault, and adjacent to it, the upheaval was particularly great–about 80 cm, which may be due to the fact that

the edge of the land block curled up when it forcibly pressed against the land mass contiguous to it.

Ignoring the local minor changes in level which must have actually occurred at the time of the great earthquake on the block surface, this large area that actually upheaved agrees in form and position with the surface of the wedge-shaped block as deduced by the stereometrical projection of the seismic foci of the Tango after-shocks.

In conclusion, the writer desires to express his sense of indebtedness to Prof. K. Suyehiro, the Director of the Earthquake Research Institute, and Professor A. Imamura in particular, under whose able and experienced guidance the present studies were made. Grateful acknowledgements are due to Messrs. K. Wakimoto, Y. Takahasi, Y. Wada, N. Arai, U. Masui, S. Sakamoto, S. Kodama, N. Hayasida and R. Yosioka, whose assistance in the arduous labour of actual seismic observations were of inestimable value.

Table VI.

(A)

Durations of the Preliminary Tremors and the Seismic Foci.

Notations;

D. P. T.=Duration of the preliminary tremors.
t_0=D. P. T. at Maiduru.
t_1=D. P. T. at Kinosaki.
t_2=D. P. T. at Ine.

Time of Occurrence.				D. P. T.			No.	Seismic Focus.		
				t_0	t_1	t_2		X	Y	Z
Month	Day	h	m	sec.	sec.	sec.		km.	km.	km.
III	12,	15	28	3·0	4·1	3·0	1	19·6	3·3	15·5
(1927)			42	3·3	3·8	3·7	2	22·7	− 3·2	15·8
		17	51	3·2	4·4	3·4	3	18·7	1·6	19·3
		18	21	2·9	5·1	4·0	4	12·8	− 4·8	20·3
			41	4·5	2·6	3·6	5	34·7	6·3	14·0
		20	03	3·0	4·3	4·4	6	18·5	−13·0	11·2
			04	3·0	4·3	4·4	7	18·5	−13·0	11·2
			35	3·3	4·1	3·6	8	21·0	− 0·9	18·2
		21	43	5·2	2·2	5·3	9	40·8	−11·3	11·3
	13,	6	30	3·6	3·5	4·0	10	25·7	− 5·2	15·2

(*to be continued.*)

Table VI. (*continued.*)

Time of Occurrence.			D. P. T.			No.	Seismic Focus.		
			t_0	t_1	t_2		X	Y	Z
Month	Day	h m	Sec.	Sec.	Sec.		km.	km.	km.
		7 44	4·1	3·0	3·1	11	30·6	8·2	13·5
		53	4·0	3·0	3·6	12	30·2	2·1	15·0
		55	4·1	3·4	3·8	13	28·8	1·7	18·9
		8 28	3·3	4·1	3·6	14	21·0	− 0·9	18·2
		10 20	5·4	3·4	4·2	15	37·6	11·2	23·0
		11 09	3·2	3.8	3·5	16	22·3	− 1·6	15·1
		25	4·3	3·1	5·1	17	31·6	−15·9	8·3
		40	4·0	4·1	3·2	18	24·6	9·7	20·8
		12 47	6·2	3·3	4·2	19	44·6	21·6	16·4
		52	2·4	4·8	2·5	20	13·0	6·4	14·1
		13 02	2·9	4·8	3·3	21	14·8	2·2	19·3
		37	4·0	3·2	4·4	22	29·2	− 8·1	14·5
		42	2·2	5·0	2·9	23	11·0	2·6	14·6
		15 26	3·2	4·2	3·0	24	20·0	5·0	17·2
		34	3·2	4·0	3·8	25	21·1	− 4·4	16·0
		18 20	4·9	3·3	4·0	26	34·5	7·6	21·4
		32	5·1	2·8	3·9	27	38·0	9·7	17·5
		20 23	6·4	3·7	5·8	28	44·2	0·0	30·8
		34	6·7	3·1	4·7	29	50·0	22·4	14·2
		23 27	3·4	4·1	3·0	30	21·6	6·4	17·7
	14,	0 47	3·5	3·7	3·7	31	24·3	− 1·7	17·0
		1 58	3·1	3·7	3·6	32	22·3	− 3·7	13·3
		2 06	3·4	4·0	3·3	33	22·0	2·9	18·1
		14	3·5	3·8	3·6	34	23·7	− 0·2	17·9
		3 53	4·1	3·2	3·8	35	29·9	1·1	17·6
		57	3·4	3·8	3·6	36	23·1	− 1·1	17·1
		5 37	4·3	3·1	3·0	37	31·5	11·5	14·0
		39	4·2	3·0	3·5	38	31·3	4·9	15·9
		6 46	4·2	3·0	3·2	39	31·3	8·3	14·5
		58	4·8	3·0	3·6	40	35·2	10·4	17·3
	14,	7 51	3·8	3·4	3·6	41	27·3	1·1	17·0
		53	3·9	3·3	3·5	42	28·3	2·9	16·8
		10 44	5·1	3·3	4·1	43	36·0	8·2	22·2
		11 20	4·1	3·0	3·6	44	30·7	2·8	15·7
		12 49	4·1	3·1	3·4	45	30·3	5·3	16·0
		13 21	3·7	3·7	3·6	46	25·2	1·2	18·5
		14 02	4·3	3·1	4·2	47	31·5	− 1·1	18·1
		16	4·7	2·6	3·9	48	36·1	4·5	16·0
		18 42	3·0	4·1	3·4	49	19·6	− 1·0	16·0
		19 13	3·0	4·1	3·3	50	19·6	0·2	16·1
		33	4·8	3·2	3·0	51	34·3	17·2	13·2
		54	3·1	4·1	3·7	52	20·1	− 3·7	16·4
		20 12	4·4	3·7	3·9	53	29·2	4·2	22·5
		22 13	4·1	3·2	3·6	54	29·8	3·3	17·2
	15,	3 08	4·0	3·2	3·8	55	29·3	0·2	16·9
		4 28	4·2	3·2	4·0	56	31·3	− 1·1	16·7
		34	5·3	2·6	4·3	57	40·2	6·3	18·4
		7 08	3·6	3·7	4·4	58	24·7	−10·1	14·7
		10 23	3·1	4·1	3·3	59	20·1	0·9	16·8
		12 05	6·1	3·0	4·2	60	45·1	19·6	15·0

(*to be continued.*)

Table IV. (*continued.*)

Time of Occurrence.			D. P. T.			No.	Seismic Focus.		
			t_0	t_1	t_2		X	Y	Z
Month	Day	h m	sec.	sec.	sec.		km.	km.	km.
		13 40	3·4	3·4	3·3	61	25·2	1·2	13·8
		46	3·2	3·9	3·8	62	21·6	− 4·6	15·6
		14 24	3·9	3·0	3·2	63	29·7	5·4	13·6
		16 12	3·8	3·2	3·3	64	28·3	4·0	15·1
		20	3·6	3·3	4·1	65	26·7	− 7·1	12·9
		20	3·4	4·0	4·2	66	22·1	− 7·9	16·7
		39	3·4	3·8	3·8	67	23·1	− 3·4	16·9
		44	3·0	4·2	3·6	68	19·1	− 2·8	16·6
		55	3·2	4·2	3·7	69	19·9	− 2·7	18·0
		20 34	3·8	3·6	3·7	70	96·3	0·5	18·5
		21 20	4·9	2·4	3·6	71	38·1	10·1	12·5
		23 32	5·9	2·7	4·9	72	44·8	5·6	21·3
	16,	3 22	3·5	3·4	3·4	73	25·7	0·7	14·8
		6 36	4·4	2·8	3·8	74	33·4	3·1	16·3
		9 31	3·5	3·8	3·4	75	23·6	2·1	17·8
		10 51	2·4	4·5	3·3	76	14·9	− 2·4	13·7
		11 05	2·3	4·6	2·9	77	13·9	1·5	13·5
		21	3·6	3·7	3·5	78	24·7	1·4	17·9
		12 01	3·2	4·0	4·3	79	21·1	−11·0	12·9
		31	4·3	3·1	3·6	80	31·5	5·1	17·4
	16,	13 39	4·2	3·3	3·4	81	29·9	6·8	17·7
		16 04	6·3	2·9	4·0	82	47·0	24·6	0·0
		51	3·6	4·0	4·0	83	25·1	− 3·7	19·5
		17 05	3·6	3·5	3·8	84	25·7	− 2·8	16·2
		12	3·8	3·2	3·3	85	28·3	4·0	13·0
		55	5·9	2·9	3·8	86	43·8	21·7	9·2
		23 55	2·8	4·0	3·6	87	19·4	− 4·9	12·8
	17,	1 29	3·1	3·8	3·9	88	21·7	− 7·1	12·9
		2 05	4·4	2·7	3·8	89	33·7	2·9	15·3
		52	4·0	3·0	3·8	90	30·1	− 0·3	15·3
		3 27	4·0	2·8	3·6	91	31·0	1·5	13·5
		4 15	4·4	3·2	4·3	92	31·7	− 2·5	19·3
		5 53	3·6	3·5	3·3	93	25·7	3·1	16·0
		6 18	3·6	3·5	3·4	94	25·7	1·9	16·1
		51	6·3	6·7	5·6	95	25·7	12·8	44·4
		7 40	5·7	2·9	3·7	96	42·3	20·4	10·7
		40	4·9	2·6	5·0	97	37·5	8·7	15·5
		14 14	3·8	3·7	4·2	98	25·7	− 5·5	18·4
		39	2·7	4·2	3·2	99	17·8	− 0·3	14·1
		17 21	6·7	4·5	5·7	100	42·6	9·6	35·8
		23	5·3	3·7	5·3	101	35·3	− 6·2	26·8
		52	3·2	3·9	3·3	102	21·6	0·9	16·1
		21 45	2·6	5·5	3·3	103	8·5	3·2	19·9
		22 40	3·4	3·3	3·6	104	25·7	− 2·6	12·7
		23 41	3·9	3·1	3·6	105	29·2	1·3	15·3
	18,	0 08	3·3	3·9	3·0	106	22·1	4·8	16·3
		2 42	4·5	2·8	3·5	107	34·0	7·6	15·2
		3 06	3·3	3·8	3·4	108	22·7	0·3	16·1
		44	5·0	2·9	3·9	109	26·9	8·7	18·4
		50	3·5	3·3	3·2	110	26·2	2·7	13·5

(*to be continued.*)

Table IV. (*continued.*)

Time of Occurrence.			D. P. T.			No.	Seismic Focus.		
			t_0	t_1	t_2		X	Y	Z
Month	Day	h m	sec.	sec.	sec.		km.	km.	km.
		4 52	3·1	3·8	3·7	111	21·7	− 4·7	13·8
		6 16	3·4	3·9	3·1	112	22·6	4·6	17·1
		9 29	3·1	3·7	3·5	113	22·3	− 2·7	13·4
		13 35	3·4	4·7	4·0	114	19·6	− 4·0	20·5
		14 40	3·9	3·4	3·5	115	27·8	3·2	17·4
		21 47	3·1	4·2	3·7	116	19·5	− 3·3	17·1
		23 45	4·5	3·2	3·3	117	32·3	10·9	16·7
	19,	4 35	3·0	4·7	3·7	119	15·9	− 2·0	19·5
		5 17	3·6	3·6	3·3	118	25·2	3·2	16·7
		6 28	3·2	4·6	2·9	120	17·4	7·4	19·2
	19,	8 10	3·1	4·5	3·4	121	17·7	1·2	19·2
		12 51	3·8	3·6	4·2	122	26·2	− 5·9	17·5
		15 50	7·4	3·8	5·7	123	53·6	19·4	25·6
		19 00	4·4	3·4	3·1	124	30·7	12·6	16·8
		54	4·8	2·9	3·2	125	35·5	14·5	13·0
		55	7·2	3·3	5·0	126	53·8	25·7	10·4
	20,	2 36	4·2	3·0	3·4	127	31·3	6·1	15·5
		3 20	3·3	3·8	4·1	128	22·7	− 8·2	14·0
		9 52	3·9	3·4	4·3	129	27·8	− 6·8	16·4
		10 54	4·2	3·4	2·8	130	29·4	13·2	14·6
		54	4·2	3·3	2·8	131	30·0	12·9	13·9
		11 27	4·9	3·3	3·8	132	34·4	8·8	20·5
		13 45	6·6	3·6	4·2	133	46·7	28·9	8·8
		14 12	6·8	3·3	4·4	134	49·9	28·0	0·0
		15 03	3·7	3·7	3·8	135	25·2	− 1·3	18·3
		22 45	4·0	3·1	3·3	136	29·7	5·6	15·1
		45	3·8	3·2	3·4	137	28·2	3·0	15·2
		47	3·7	3·6	3·1	138	25·7	6·4	16·7
	21,	0 11	5·1	3·7	4·0	139	33·8	10·8	24·1
		2 54	3·5	3·5	3·1	140	25·2	4·2	15·0
		11 49	3·7	3·4	3·0	141	26·6	6·7	14·9
		22 21	5·3	2·7	4·3	142	39·9	6·7	19·1
	22,	0 46	4·5	3·4	4·1	143	31·3	1·9	21·6
		2 17	6·7	2·0	4·9	144	54·2	16·4	0·0
		3 16	6·5	3·3	4·8	145	47·3	17·8	21·4
		5 16	2·3	4·3	3·0	146	15·8	− 0·6	11·4
		6 54	5·0	3·3	3·7	147	35·1	12·1	19·8
		12 57	3·7	3·3	3·2	148	27·1	4·4	14·8
		15 18	3·6	3·7	4·2	149	24·6	− 7·2	16·3
		16 58	3·5	3·8	3·5	150	23·6	1·0	17·8
		20 55	3·7	3·5	2·7	151	26·2	9·7	14·2
	23,	1 29	2·3	3·8	3·7	152	18·7	− 8·0	0·0
		4 48	3·8	3·2	3·4	153	28·2	3·0	15·2
		5 55	5·3	3·0	4·9	154	38·6	− 1·5	22·5
		18 52	2·5	4·4	3·1	155	15·8	0·1	14·0
		21 58	4·1	2·7	4·3	156	31·9	− 6·8	11·6
		22 50	3·7	3·5	2·8	157	26·1	8·9	14·6
	24,	1 56	3·2	3·7	3·4	158	22·7	− 0·6	14·7
		6 40	4·0	3·2	3·6	159	29·2	2·5	16·7
		8 41	3·5	3·8	3·2	160	23·6	4·2	17·3

(*to be continued.*)

Table IV. (*continued.*)

Time of Occurrence.			D. P. T.			No.	Seismic Focus.		
			t_0	t_1	t_2		X	Y	Z
Month	Day	h m	sec.	sec.	sec.		km.	km.	km.
	24,	8 56	2·2	5·7	2·8	161	5·6	6·6	16·4
		10 18	3·3	3·7	3·4	162	23·2	0·2	15·5
		33	3·2	3·7	3·4	163	22·7	− 0·6	14·7
		17 39	3·0	3·9	3·5	164	20·7	2·6	14·3
	25,	0 34	5·5	2·9	4·2	165	40·6	11·4	19·3
		4 14	3·9	3·6	3·0	166	26·8	9·2	16·8
		9 17	4·4	2·8	4·2	167	33·4	− 2·0	16·2
		13 36	4·2	2·8	3·5	168	32·0	4·4	14·4
		14 16	5·6	2·1	4·3	169	44·2	9·5	13·7
		17 40	3·2	4·0	3·1	170	21·1	3·4	16·4
		19 13	4·4	2·7	3·4	171	33·7	7·6	13·6
		48	4·0	4·3	3·9	172	23·3	2·3	24·2
		23 33	3·5	4·0	4·3	173	22·5	− 8·4	17·2
	26,	7 56	3·0	4·2	3·0	174	19·0	0·6	16·7
	27,	1 21	6·1	3·2	3·6	175	43·6	26·6	0·0
		3 21	4·0	3·0	3·5	176	30·2	3·1	15·0
		4 03	2·9	4·9	3·0	177	14·1	5·7	19·3
		19 54	4·1	3·2	4·2	178	29·8	− 4·0	17·0
	28,	8 53	7·5	2·0	6·0	179	62·2	11·2	6·0
	29,	0 52	4·0	3·3	3·9	180	28·8	− 0·9	17·7
		5 06	5·1	2·6	3·9	181	38·8	9·3	16·2
		22 02	3·8	3·1	3·6	182	28·6	0·4	14·5
	30,	2 18	5·3	3·3	3·8	183	37·3	14·8	19·7
		4 23	5·1	2·8	5·7	184	38·0	−18·1	8·7
		10 23	4·2	3·3	4·4	185	30·0	− 5·6	18·2
		22 30	3·0	5·3	3·1	186	11·7	7·0	21·4
		39	2·4	5·3	3·2	187	9·4	2·2	17·8
		39	2·4	5·3	3·2	188	9·4	2·2	17·8
		41	2·3	5·8	3·2	189	5·1	3·8	18·4
		57	2·3	6·0	3·3	190	3·5	3·7	18·8
		23 18	2·1	6·0	3·3	191	2·9	2·7	17·2
	31,	0 53	2·7	5·3	3·6	192	10·5	− 0·6	20·2
		3 35	5·3	2·3	5·3	193	41·4	− 9·5	14·3
		9 09	4·5	3·8	3·5	194	29·4	10·6	21·8
		13	7·5	2·8	6·3	195	59·4	6·4	21·0
		11 44	7·7	4·0	6·5	196	56·0	9·6	32·0
		12 14	4·4	3·5	3·5	197	30·4	8·5	19·8
		19 13	3·4	3·8	3·8	198	23·0	− 3·4	16·8
IV	1,	2 56	3·1	4·2	3·8	199	19·5	− 4·6	16·9
		4 40	3·6	4·1	3·7	200	22·4	0·4	20·5
	1,	6 07	2·6	4·8	3·6	201	13·8	− 3·2	17·0
		9 49	2·5	4·5	3·6	202	15·2	− 5·1	13·6
		11 42	3·9	2·9	4·2	203	30·0	− 6·6	12·0
		14 49	2·3	4·9	3·4	204	11·9	− 2·4	15·2
		16 26	2·2	4·8	2·9	205	12·2	1·7	13·8
		18 23	2·3	4·9	2·9	206	12·0	2·8	15·1
		19 24	2·6	4·6	3·0	207	15·0	− 4·0	15·5
		20 28	5·0	2·7	4·6	208	37·8	− 1·3	18·9
	2,	6 28	4·2	3·8	4·3	209	27·6	− 2·9	22·2
		10 29	2·1	5·3	3·4	210	8·4	− 1·8	15·4

(*to be continued.*)

Table IV. (*continued.*)

Time of Occurrence.			D. P. T.			No.	Seismic Focus.		
			t_0	t_1	t_2		X	Y	Z
Month	Day	h m	sec.	sec.	sec.		km.	km.	km.
		11 35	2·6	5·0	3·3	211	12·3	0·9	18·2
		23 18	2·2	4·9	3·6	212	11·6	− 5·2	13·6
	3,	0 05	2·3	4·7	3·5	213	13·3	− 4·3	13·5
		1 34	2·3	5·3	3·8	214	9·1	− 5·5	16·2
		2 07	2·2	5·1	3·7	215	10·3	− 5·6	14·5
	7,	4 47	4·4	3·8	4·5	216	28·8	− 3·5	23·5
		5 37	5·4	3·1	3·6	217	39·0	18·0	15·2
	8,	13 26	6·3	3·2	4·2	218	46·1	23·4	12·8
		17 42	2·1	5·8	3·4	219	4·5	0·6	17·1
	11,	18 54	3·7	3·8	3·6	220	24·7	1·6	19·1
	12,	4 19	2·5	5·1	3·6	221	11·3	− 2·6	17·8
		5 06	2·5	5·0	3·7	222	11·9	− 4·2	16·9
		9 33	5·0	2·2	3·6	223	39·4	10·9	10·3
		21 58	3·2	4·7	3·3	224	16·8	3·8	20·8
		22 19	2·7	5·1	3·0	225	11·9	5·0	18·7
		57	3·0	4·2	3·4	226	19·0	− 0·6	16·6
	13,	0 28	3·6	3·4	4·0	227	26·2	− 5·6	14·3
		7 06	4·7	3·0	4·3	228	34·5	0·4	19·7
		17 55	6·4	2·2	4·6	229	50·6	16·6	8·2
		21 00	3·2	4·0	3·2	230	21·2	2·4	16·6
		52	3·0	5·0	3·5	231	13·9	1·4	21·2
	14,	1 17	5·0	2·5	4·3	232	38·4	2·6	17·2
		2 43	2·5	5·0	3·2	233	11·9	1·5	17·4
		5 57	3·0	4·2	3·6	234	19·1	− 2·9	16·4
		12 36	5·3	4·0	4·2	235	33·8	11·9	26·9
		21 20	4·8	2·5	3·6	236	37·1	9·4	13·4
	15,	1 59	2·6	3·9	3·5	237	19·2	− 5·3	9·4
		2 44	4·0	3·1	3·5	238	29·7	3·4	15·7
		3 51	3·5	4·3	3·5	239	20·8	2·6	20·9
		4 04	3·0	4·5	3·6	240	17·2	− 1·7	18·5
	15,	4 56	3·6	4·0	4·2	241	23·0	− 6·2	18·9
		10 49	5·0	2·3	4·3	242	39·1	2·4	15·7
		14 36	2·3	6·1	3·4	243	2·6	3·2	19·0
	16,	4 52	3·5	3·4	3·2	244	25·6	3·1	14·3
		20 57	4·2	3·0	3·6	245	31·3	3·9	16·2
		21 08	3·1	4·4	3·3	246	18·2	2·1	18·7
		22 34	4·5	2·8	4·2	247	34·0	− 0·8	17·0
	17,	15 23	3·7	4·2	3·6	248	22·4	2·9	21·6
		44	3·7	4·2	3·5	249	22·4	4·0	21·4
	18,	9 39	4·6	3·1	3·6	250	33·4	8·6	18·0
		18 03	4·0	3·3	3·0	251	28·8	9·2	15·1
		20 24	7·1	3·5	7·0	252	54·2	−10·6	27·5
	20,	5 49	2·1	6·0	3·6	253	2·8	− 0·6	17·4
	21,	4 50	5·0	2·8	3·8	254	37·3	9·9	17·1
		5 32	2·4	4·7	3·6	255	13·5	− 4·8	14·3
		11 23	3·1	3·8	3·3	256	21·7	0·0	14·6
		16 43	3·9	3·4	3·8	257	27·8	− 0·2	17·7
	22,	12 31	4·3	3·0	4·1	258	31·9	− 1·2	17·2
		22 35	3·4	4·2	3·6	259	20·9	0·2	19·8
		23 32	7·2	3·2	6·5	260	54·6	− 1·8	22·8

(*to be continued.*)

Table VI. (*continued.*)

Time of Occurrence.			D. P. T.			No.	Seismic Focus.		
			t_0	t_1	t_2		X	Y	Z
Month	Day	h m	sec.	sec.	sec.		km.	km.	km.
	23.	0 40	3·5	4·4	3·7	261	20·2	0·6	21·6
	24,	15 45	5·3	3·0	4·1	262	38·7	10·2	20·0
	25,	19 27	3·1	3·7	4·2	263	22·3	−11·3	7·8
		22 08	4·1	3·3	3·2	264	29·3	8·2	16·4
	26,	4 36	3·8	4·5	3·5	265	21·0	5·9	23·4
		22 10	3·5	3·9	3·2	266	23·1	1·7	18·0
		23 38	3·9	3·6	3·7	267	26·8	1·5	19·1
		38	5·3	2·3	3·9	268	41·3	11·3	13·0
	27,	2 03	5·3	2·7	3·1	269	39·3	20·5	0·0
		8 07	6·3	4·0	6·1	270	42·0	− 5·9	32·2
		19	3·9	4·1	3·6	271	24·1	4·4	22·1
	28,	2 04	3·0	4·2	3·6	272	19·1	− 2·9	16·4
		8 37	7·5	4·0	5·3	273	53·6	28·8	17·6
		16 26	5·5	3·6	3·1	274	37·4	26·3	8·2
		18 04	2·6	3·8	2·9	275	19·8	0·4	9·6
	29,	9 03	4·2	3·2	3·9	276	30·4	0·8	18·2
		21	3·6	3·3	3·7	277	26·6	− 2·1	14·5
	30,	7 51	4·2	3·0	3·2	278	31·3	8·4	14·4
		12 18	3·6	3·4	3·6	279	26·1	− 0·6	15·4
		13 30	5·2	2·8	4·8	280	38·7	− 1·6	20·5
V	1,	0 28	3·9	3·6	3·6	281	26·8	2·8	19·0
		2 46	3·1	3·1	4·0	282	25·2	− 8·8	0·0
		3 26	4·6	5·9	5·6	283	15·6	−10·8	33·9
		8 48	3·8	4·2	3·8	284	23·0	1·3	22·4
		20 09	2·5	4·3	2·9	285	16·5	1·5	13·0
	2,	21 06	3·5	3·8	3·4	286	23·6	2·0	17·7
	3,	11 48	4·5	2·8	3·8	287	34·0	4·4	16·5
	4,	9 01	3·1	3·9	3·0	288	21·2	3·3	15·0
		10 57	4·0	3·8	3·7	289	26·2	3·1	21·0
	5,	6 13	4·3	3·0	3·5	290	31·9	6·3	16·2
		7 04	5·7	1·6	5·4	291	46·4	− 7·2	10·7
	6,	6 33	4·1	3·3	3·5	292	29·4	4·9	17·6
		17 19	3·6	3·0	2·9	293	28·0	5·6	10·4
	7,	8 13	4·2	2·8	4·5	294	32·1	4·6	14·4
		54	4·8	4·5	3·5	295	27·1	16·4	25·3
		9 00	2·4	5·4	3·0	296	8·6	4·6	17·8
		19 28	5·0	3·0	4·1	297	36·5	6·6	20·1
		39	3·4	4·0	3·6	298	22·0	− 0·5	18·4
		21 15	3·0	4·3	2·9	299	18·5	4·8	16·6
	8,	6 02	4·5	2·5	4·0	300	35·1	1·0	14·6
		9 07	4·5	2·4	4·3	301	35·4	− 3·1	13·4
		11 44	3·7	3·3	3·2	302	27·2	4·4	14·7
		12 44	3·5	3·9	3·7	303	23·1	− 1·1	18·4
		17 06	3·4	3·9	3·4	304	22·6	1·6	17·6
	9,	3 13	1·4	6·0	3·6	305	1·2	− 3·6	11·2
		5 39	4·0	3·2	3·8	306	29·3	0·0	16·8
		7 33	3·6	4·8	2·9	307	18·2	11·6	21·5
		15 55	2·6	4·6	2·8	308	15·0	4·3	15·4
		21 01	3·5	4·3	3·8	309	20·8	− 0·9	20·9
	10,	1 05	4·2	2·6	3·9	310	32·8	− 0·6	13·2

(*to be continued.*)

Table IV. (*continued.*)

Time of Occurrence.				D. P. T.			No.	Seismic Focus.		
				t_0	t_1	t_2		X	Y	Z
Month	Day	h	m	sec.	sec.	sec.		km.	km.	km.
			33	4·4	2·5	3·6	311	34·4	4·8	13·0
			35	4·7	2·3	4·0	312	37·0	2·9	13·8
	11,	2	30	3·1	4·0	3·4	313	20·7	− 0·6	16·0
	12,	19	50	3·5	3·5	2·8	314	25·2	7·0	13·8
	13,	17	43	4·1	3·6	3·6	315	27·9	4·5	19·9
	14,	0	01	4·2	2·7	4·5	316	32·5	− 8·7	11·0
		19	24	5·0	5·0	3·8	317	25·2	17·0	29·3
	16,	3	29	3·2	3·2	3·8	318	25·2	− 7·0	6·6
		11	25	2·7	4·5	2·9	319	16·0	3·6	15·8
		22	57	2·1	5·0	2·9	320	10·7	1·9	14·0
	17,	21	42	4·2	3·0	3·4	321	31·2	6·1	15·4
		23	52	3·1	4·2	2·6	322	19·5	7·9	15·5
	20,	16	51	5·8	3·0	4·2	323	42·8	15·6	18·2
			52	6·2	2·5	4·3	324	47·8	18·8	9·4
		19	21	5·8	2·2	5·2	325	45·6	− 1·5	17·9
	23,	1	36	4·7	3·2	3·4	326	33·6	12·1	17·3
			55	4·7	2·7	3·3	327	35·6	12·2	12·5
		22	18	2·4	5·1	2·8	328	11·0	5·0	16·4
	24,	21	08	6·0	3·2	4·7	329	43·2	15·4	23·4
		23	01	6·0	2·1	5·2	330	47·5	1·4	17·4
	25,	3	27	3·2	4·1	3·1	331	21·1	3·4	16·4
	27,	6	34	6·0	1·1	5·3	332	49·6	− 2·2	9·0
		11	15	3·9	3·4	3·6	333	37·7	2·3	17·5
		17	35	5·9	1·3	5·0	334	48·5	2·0	10·6
	28,	1	41	4·0	3·2	3·8	335	29·3	0·0	16·8
	29,	1	30	6·1	1·1	5·0	336	50·6	4·5	8·0
			30	3·4	3·5	3·8	337	24·7	− 4·4	13·7
		4	32	5·1	1·1	5·6	338	49·0	− 8·4	3·6
VI	6,	9	12	6·0	2·6	4·8	339	45·7	8·5	19·6
		10	45	4·4	3·2	3·7	340	31·7	5·5	18·6
	7,	3	12	4·9	2·6	4·3	341	36·2	2·5	19·8
	8,	12	51	4·4	3·4	4·0	342	30·6	2·2	20·6
	9,	7	58	3·4	3·8	3·2	343	23·2	3·3	16·5
	11,	3	35	5·0	3·4	4·3	344	34·6	4·8	23·4
	13,	4	03	3·8	3·2	3·1	345	28·2	6·0	14·0
	14,	2	46	4·2	3·2	4·7	346	30·4	−10·3	14·7
	15,	3	06	2·8	3·6	3·6	347	21·5	− 6·2	7·2
		8	28	5·9	3·8	3·9	348	39·5	23·2	19·4
	17,	18	30	3·4	3·6	3·1	349	24·2	3·7	14·8
	18,	7	02	4·7	2·6	3·7	350	36·0	7·2	15·0
	19,	18	33	2·7	4·5	3·6	351	16·0	− 3·7	15·7
		21	24	4·1	3·2	3·9	352	29·8	− 0·3	17·3
	22,	10	33	3·5	3·5	3·9	353	25·2	− 3·6	14·9
	24,	19	42	6·0	2·9	3·8	354	44·6	23·2	4·9
	25,	20	19	5·8	3·7	3·2	355	39·1	29·3	0·0
VII	2,	0	27	6·4	3·0	5·7	356	49·5	3·4	25·0
	4,	4	42	5·4	2·1	4·9	357	42·7	− 2·3	15·8
	5,	23	50	3·5	3·6	3·2	358	24·7	3·4	15·6
	6,	3	05	3·8	2·9	3·0	359	29·4	6·2	11·0
		6	41	4·5	3·2	5·3	360	32·3	−16·4	10·8

(*to be continued.*)

Table VI. (*continued.*)

Time of Occurrence.				D. P. T.			No.	Seismic Focus.		
				t_0	t_1	t_2		X	Y	Z
Month	Day	h	m	sec.	sec.	sec.		km.	km.	km.
	7,	5	24	2·4	5·3	2·7	361	9·4	6·8	16·6
			34	5·1	2·7	4·1	362	38·4	6·9	18·0
	11,	22	37	5·0	4·4	3·3	363	29·2	20·5	22·4
	13,	1	02	5·5	4·4	3·5	364	32·8	24·4	21·8
	16,	12	28	6·9	3·9	6·2	365	48·0	2·3	32·8
	20,	7	20	6·9	3·9	6·2	366	48·0	2·3	32·8
	21,	0	57	4·3	2·6	3·5	367	33·4	4·9	13·0
		12	37	4·3	2·7	3·6	368	33·0	4·3	14·1
	23,	7	08	4·6	2·6	3·6	369	35·4	7·2	14·2
	24,	9	23	2·8	4·7	2·7	370	15·1	6·8	16·8
		12	24	2·8	4·7	2·7	371	15·1	6·8	16·8
		13	55	3·6	3·6	4·0	372	25·2	− 4·9	16·1
VIII	4,	7	38	4·2	2·8	4·4	373	32·0	− 7·0	13·0
	5,	11	44	4·3	3·0	3·3	374	31·8	8·3	15·0
		21	40	5·1	2·6	4·4	375	38·8	2·6	18·4
	6,	13	31	5·1	2·6	3·3	376	38·8	16·3	8·8
	7,	0	20	3·4	3·3	3·4	377	25·7	− 0·3	12·7
		19	39	1·6	6·3	2·9	378	−1·0	5·9	12·1
	10,	0	33	4·4	3·8	3·7	379	28·7	7·1	22·4
		10	31	4·6	4·1	3·8	380	28·3	9·1	25·0
	19,	12	45	5·4	2·7	4·6	381	40·6	3·8	20·2
		23	02	3·0	3·9	3·9	382	20·8	− 7·6	12·2
	23,	19	02	4·3	2·7	3·2	383	33·0	8·6	12·0
	30,	23	03	4·0	3·2	3·7	384	29·3	1·4	16·7
IX	17,	4	04	3·0	4·2	3·8	385	19·1	− 5·2	15·7
	18,	7	17	4·1	3·4	3·9	386	28·8	0·3	19·0
	23,	2	17	4·4	4·4	3·6	387	25·2	10·6	25·2
		5	11	3·5	3·0	4·0	388	27·5	− 7·4	7·8
			12	3·9	3·5	3·4	389	27·3	4·7	17·7
			18	3·5	3·2	3·9	390	26·6	− 5·8	11·2
		21	54	5·0	3·0	4·8	391	36·4	− 3·6	20·8
	25,	5	59	5·0	2·7	5·8	392	37·8	−19·6	0·0
		6	09	5·0	2·7	5·8	393	37·8	−19·6	0·0
	27,	8	38	2·0	4·5	2·1	394	13·7	6·2	7·8
X	3,	8	29	6·3	3·3	5·2	395	45·5	8·2	26·0
	14.	12	37	3·6	2·8	3·7	396	28·8	− 3·3	8·9
	22,	3	57	4·4	3·6	3·6	397	29·8	7·7	20·8
	24,	7	57	2·7	4·0	3·2	398	19·0	− 1·1	12·4
	29,	7	46	2·8	3·9	3·6	399	20·0	− 5·2	11·6
XI	10,	11	47	4·0	3·5	4·3	400	27·8	− 5·6	18·1
	12,	0	02	3·9	2·8	2·9	401	30·4	7·9	10·0
	16,	20	29	5·4	2·7	3·6	402	40·6	16·9	11·8
	22,	15	31	2·7	3·5	2·3	403	21·8	5·2	4·7
	26,	20	10	5·3	2·7	3·9	404	39·8	11·9	16·3

Table VI.

(B)

Durations of the Preliminary Tremors and the Seismic Foci.

Notations;

D. P. T.=Duration of the preliminary tremors.
t_0=D. P. T. at Maiduru.
t_1=D. P. T. at Kinosaki.
t_2=D. P. T. at Kobe-mura.
t_3=D. P. T. at Taiza.

Time of Occurrence.				D. P. T.				No.	Seismic Focus.		
				t_0	t_1	t_2	t_3		X	Y	Z
Month	Day	h	m	sec.	sec.	sec.	sec.		km.	km.	km.
XII	28,	12	35	5·5	2·3	2·6		405	42·8	12·0	13·3
	29,	20	42	3·6	3·7	2·6		406	24·6	− 6·8	16·3
	30,	13	52	6·1	2·9	3·0		407	45·6	23·7	0·0
I	4,	1	34	2·4	4·1	1·5		408	17·4	5·0	9·1
	10,	12	32	2·4	3·8	1·6		409	19·1	− 1·8	6·6
	25,	7	10	3·3	3·2	0·9		410	25·7	7·4	7·8
		20	21	3·4	3·2	0·9		411	26·2	8·8	7·7
	30,	5	01	2·5	3·6	1·4	3·0	412	20·4	− 0·8	6·0
		18	14	5·1	2·8	2·3	1·7	413	38·4	16·8	12·2
II	6,	9	21	3·0		0·5	2·3	414	25·0	3·1	0·0
	8,	23	40	3·1		1·4	2·4	415	22·3	7·3	11·2
	12,	21	27	5·0	3·0	2·2	1·6	416	36·3	17·1	12·0
	14,	20	48	4·0	2·8	1·7	2·8	417	30·6	1·4	11·2
	18,	18	49	5·0	2·6	2·3	2·4	418	37·7	9·2	14·8
			49		2·0	2·1	2·6	419	38·8	3·9	11·4
	19,	5	27	3·3	3·3	1·2	2·0	420	25·2	8·9	10·3
	20,	3	45	3·0		0·5	2·3	421	25·0	3·1	0·0
	23,	7	30		3·2	1·0	2·2	422	25·5	5·9	8·2
	26,	7	33		2·6	2·7	1·4	423	43·8	21·3	0·0
	29,	10	38	3·0	3·6	2·0	3·3	424	23·3	− 1·5	13·8
III	1,	22	34	5·5	2·0	2·7	2·9	425	43·0	5·1	13·9
	4,	22	54		2·6	1·8	2·2	426	34·3	7·8	12·6
	5,	17	59		2·6	1·2	1·2	427	33·2	12·6	5·1
	23,	12	43	3·0	3·2		1·5	428	24·2	10·0	0·0
		18	01		2·7	2·5	2·2	429	39·7	13·4	14·9
	27,	8	06		3·0	2·1	2·2	430	33·8	11·2	15·4
		23	10		3·3	1·7	1·5	431	30·3	15·5	11·2
IV	6,	1	49	5·4	2·6		2·3	432	41·0	13·0	14·8
	9,	9	01	2·6	3·5	0·8		433	21·3	3·9	3·0
	22,	3	20	3·0		1·5	1·8	434	18·3	16·7	5·0
V	5,	6	41	4·0	2·9		1·6	435	30·4	11·2	9·0
			41	4·7	3·0		2·0	436	34·4	13·1	14·6
	28,	3	15		2·9	1·1	1·6	437	29·6	5·6	7·9
	29,	0	04	3·3		1·0	2·0	438	25·2	8·2	8·4
VI	1,	8	34		3·0	2·4	1·8	439	37·7	17·2	13·4

(to be continued.)

Table VI. (B) (*continued.*)

Time of Occurrence.			D. P. T.				No.	Seismic Focus.		
			t_0	t_1	t_2	t_3		X	Y	Z
Month	Day	h m	sec.	sec.	sec.	sec.		km.	km.	km.
	7,	6 31		2·6	1·5	1·5	440	34·2	12·2	8·4
	9,	23 52	5·5	1·5		2·9	441	44·9	3·6	10·8
	16,	12 06	3·0	3·5	0·9	2·2	442	23·0	6·8	6·7
	20,	17 26	5·4		2·3	1·8	443	42·7	13·6	7·6
		29	3·2		2·0	2·2	444	17·3	17·5	10·9
VII	9,	0 19	3·3		0·5	2·0	445	27·0	5·5	3·4
	14,	15 01	3·9		1·5	2·7	446	31·9	− 0·2	7·7

Table VII. Seismic Foci in Region III.

No. of Earthq.	X′	No. of Fig.	Y′	No. of Fig.	Focal Depth.
	km.		km.		km.
8	0·3		0·1		18·3
10	6·7		0·7		15·2
12	4·1		8·9		15·0
13	3·6		7·6		18·9
14	0·3		0·1		18·1
16	1·7		0·6		15·1
18	− 5·3		10·0		20·8
22	11·2		1·3		14·5
30	− 4·8		5·5		17·7
31	3·1		2·0		17·0
33	− 1·9		3·4		18·1
34	1·6		2·6		17·9
35	4·8		8·0		17·6
36	1·8	26	1·5		17·1
38	2·9		11·7		15·9
41	3·0		6·1	33	17·0
42	2·3		8·1		16·8
44	4·0		9·8		15·7
45	1·9		11·2		16·0
46	1·5		4·7		18·5
47	7·5		7·8		18·1
53	1·9		9·6		22·5
54	3·1		9·4		17·2
55	5·0		7·0		16·9
56	7·3		7·6		16·7
61	1·5		4·6		13·8
63	1·4		10·8		13·6
64	1·5		8·8		15·1
65	8·7		0·1		12·9
70	2·7		5·0		18·5
73	2·1		4·6		14·8
74	5·6	27	12·0		16·3
75	− 0·3		4·1		17·8
78	1·0		4·4		17·9
80	2·8		11·9		17·4

(*to be continued.*)

Table VII. (*continued.*)

No. of Earthq.	X′	No. of Fig.	Y′	No. of Fig.	Focal Depth.
	km.		km.		km.
81	0·5		11·9		17·7
84	4·8		2·3		16·2
85	1·5		8·8		15·0
89	5·9		12·1		15·3
90	5·9		7·2	33	15·3
91	5·2		9·1		13·5
92	8·6		7·0		19·3
93	0·4		6·3		16·0
94	1·3		5·5		16·1
98	6·8		0·5		18·4
102	− 0·7		1·9		16·1
104	4·7		2·5		12·7
105	4·1		7·8		15·3
106	− 3·3		4·8		16·3
108	0·2		2·1		16·1
110	1·0		6·5		13·5
112	− 2·8		5·1		17·1
115	1·7		7·9		17·4
119	0·0		6·1		16·7
122	7·4		0·6		17·5
129	9·2		1·2		16·4
135	3·3		3·0		18·3
136	1·3	27	11·0		15·1
137	2·2		8·2		15·2
138	− 2·1		8·6		16·7
140	− 0·8		6·7		15·0
141	− 1·7		9·5		14·9
143	5·1		9·7	34	21·6
148	0·4		8·3		14·8
150	0·6		3·4		17·8
151	− 4·2		11·2		14·2
153	2·2		8·2		15·1
156	11·9		4·3		11·6
157	− 3·6		10·6		14·6
158	1·1		1·6		14·7
159	3·2		8·5		16·7
160	− 1·8		5·6		17·3
162	0·8		2·5		15·5
163	1·1		1·6		14·7
164	− 2·6		2·3		14·3
166	− 3·4		11·3		16·8
167	9·4		8·6		16·2
168	3·7		11·9		14·4
170	− 2·9		3·2		16·4
172	− 0·6		4·1		24·2
176	3·5		9·7		15·0
178	8·4		4·6		17·0
180	5·5		6·0		17·7
182	4·4		6·7		14·5
185	9·8		3·7		18·2

(*to be continued.*)

Table VII. (*continued.*)

No. of Earthq.	X′	No. of Fig.	Y′	No. of Fig.	Focal Depth.
	km.		km.		km.
200	0·5		2·3		20·5
203	10·6		2·8		12·0
208	11·9		12·2		18·9
209	6·2		3·6		22·2
216	7·4		4·1		23·5
220	0·9		4·5		19·1
227	7·3		0·7		14·3
228	8·4		10·9		19·7
230	− 2·1		2·5		16·6
238	2·9		9·4		15·7
239	− 2·5		2·3		20·9
244	0·4		6·2		14·3
245	3·6		10·9		16·2
247	8·9		9·8		17·0
248	− 1·7	28	3·7	35	21·6
249	− 2·5		4·4		21·4
256	0·0		1·2		14·6
257	4·3		5·6		17·7
258	7·8		7·9		17·2
259	− 0·6		0·7		19·8
261	− 1·4		0·5		21·6
265	− 4·9		4·7		23·4
266	− 2·5		5·4		18·0
267	2·4		6·0		19·1
271	− 1·7		6·0		22·1
276	5·3		8·2		18·2
277	4·9		3·4		14·5
279	3·5		4·1		15·4
281	1·4		7·0		19·0
284	0·0		3·1		22·4
286	− 0·2		4·0		17·7
288	− 2·7		3·1		15·0
289	0·8		6·7		21·0
292	1·6		10·3		17·6
293	− 0·3		10·1		10·4
294	3·6		12·1		14·4
298	0·6		1·2		18·4
300	8·3		11·9		14·6
301	11·6	29	9·3		13·4
302	0·5		8·3	36	14·7
303	1·8		1·6		18·4
304	− 0·5		3·0		17·6
306	5·2		6·9		16·8
310	8·0		9·1		13·2
313	− 0·2		0·1		16·0
314	− 2·8		8·6		13·8
315	0·9		8·9		19·9
321	1·9		12·4		15·4
331	− 2·9		3·1		16·4
335	5·2		6·9		16·8

(*to be continued.*)

Table VII. (*continued.*)

No. of Earthq.	X′	No. of Fig.	Y′	No. of Fig.	Focal Depth.
	km.		km.		km.
337	5·3		0·5		13·7
340	2·7		12·3		18·6
342	4·5		9·3		20·6
343	− 1·4		4·6		16·5
345	0·0		10·1		14·0
349	− 1·0		5·6		14·8
352	5·7		7·0		17·3
353	5·0		1·4	36	14·9
358	− 0·5	30	5·8		15·6
359	0·6		11·1		11·0
368	4·5		12·5		14·1
372	6·0		0·5		16·1
377	3·0		4·0		12·7
379	− 0·5		11·2		22·4
380	− 2·3		12·3		25·0
384	4·1		7·8		16·7
386	4·6		6·7		19·0
388	9·4		0·5		7·8
389	0·3		8·6		17·7
390	7·2		0·9		11·2
396	7·3		4·2		8·9
400	8·3		2·0		18·1
403	− 3·8		4·8		4·7
410	− 2·8		9·2		7·8
411	− 3·5		10·6		7·7
414	0·0		5·8		0·0
415	− 5·0		6·6		11·2
417	5·0		8·8		11·2
420	− 4·3	31	9·9	37	10·3
421	0·0		5·8		0·0
422	− 1·8		8·1		8·2
424	2·2		1·4		13·8
428	− 5·8		9·9		0·0
433	− 3·2		3·6		3·0
437	1·2		10·9		7·9
438	− 3·7		9·4		8·4
442	− 4·2		6·8		6·7
445	− 0·5		8·9		3·4
446	7·0		8·7		7·7

Table VIII. Seismic Foci in Region II.

No. of Earthq.	X″	No. of Fig.	Y′	No. of Fig.	Focal Depth.
	km.		km.		km.
5	4·0		2·7		14·0
11	− 0·2		0·9		13·5
15	2·4	39	8·2	43	23·0
26	2·9		3·4		21·4
27	3·7		7·4		17·5

(*to be continued.*)

Table VIII. (*continued.*)

No. of Earthq.	X″	No. of Fig.	Y′	No. of Fig.	Focal Depth.
	km.		km.		km.
37	1·9		3·8		14·0
39	0·2		1·5		14·5
40	1·4		5·8		17·3
43	3·5		4·9		22·2
48	6·3		2·5		16·0
57	7·7		6·7		18·4
71	3·5		7·8		12·5
72	11·3		9·7		21·3
97	4·1		6·4		15·5
107	2·6		3·0		15·2
109	3·8		6·0		18·4
117	−0·9	39	4·0	43	16·7
124	−3·3		4·0		16·8
125	−1·4		8·8		13·0
127	1·9		0·0		15·5
130	−4·6		3·4		14·6
131	−3·9		3·6		13·9
132	2·0		4·1		20·5
139	0·2		5·1		24·1
142	7·3		6·8		19·1
147	0·1		6·9		19·8
171	0·4		2·8		13·6
181	4·6		7·8		16·2
194	−2·7		1·6		21·8
197	−0·4		1·0		19·8
223	3·8		9·3		10·3
232	9·3		2·9		17·2
236	3·4		6·5		13·4
242	9·9		3·3		15·7
250	1·5		3·3		18·0
251	−2·0		0·3		15·1
254	3·1		7·1		17·1
262	3·8		8·3		20·0
264	−0·9		0·0		16·4
278	0·2		1·6		14·4
287	5·0		0·8		16·5
290	2·2		0·5		16·2
297	5·1		4·1		20·1
311	5·0	40	1·3	44	13·0
312	8·1		2·0		13·8
326	−0·9		5·8		17·3
327	0·3		7·3		12·5
333	9·1		2·1		17·5
341	7·9		1·2		19·8
344	5·1		1·5		23·4
350	4·3		4·2		15·0
362	6·2	41	5·8		18·0
367	4·2		0·7		13·0
369	3·9		3·7		14·2
374	0·7		1·8		15·0

(*to be continued.*)

Table VIII. (*continued.*)

No. of Earthq.	X″	No. of Fig.	Y′	No. of Fig.	Focal Depth.
	km.		km.		km.
375	9·6		3·2		18·4
381	9·9		5·3		20·2
383	1·2		2·9		12·0
397	−0·2		0·0		20·8
401	0·1		0·6		10·0
418	3·9		6·8		14·8
419	8·6		4·0		11·4
425	10·6	41	7·9		13·9
426	2·7		3·3		12·6
427	−1·6		5·8	45	5·1
430	−0·2		5·3		15·4
431	−5·7		5·6		11·2
435	−2·4		2·8		9·0
436	−1·2		7·0		14·6
440	−0·6		6·2		8·4

Table IX. Seismic Foci in Region I.

No. of Earthq.	X‴	No. of Fig.	Y″	No. of Fig.	Focal Depth.
	km.		km.		km.
19	1·0		10·4		16·4
29	4·6		14·4		14·2
51	−4·3		0·5		13·2
60	2·6		9·1		15·0
82	1·0		14·3		0·0
86	0·3		9·9		9·2
96	−0·6		8·0		10·7
123	9·4		14·2		25·6
126	5·6		19·3		10·4
133	−1·9		17·4		8·8
134	1·1		18·3		0·0
144	11·8		12·3		0·0
145	5·5		9·1		21·4
169	8·3		0·6		13·7
175	−2·9	47	13·7	48	0·0
183	−0·4		0·4		19·7
217	−1·1		4·1		15·2
218	1·1		12·7		12·8
229	8·8		10·1		8·2
268	4·9		0·2		13·0
269	−2·4		5·3		0·0
323	3·4		4·5		18·2
324	5·3		10·2		0·4
329	6·3		1·5		23·4
339	10·1		0·7		19·6
348	−3·9		8·4		19·4
354	0·0		11·6		4·9
376	−0·2		2·5		8·8
402	0·9		4·2		11·8
405	5·7		1·7		13·3

(*to be continued.*)

Table IX. (*continued.*)

No. of Earthq.	X‴	No. of Fig.	Y″	No. of Fig.	Focal Depth.
	km.		km.		km.
407	0·5		12·6		0·0
413	−0·8		2·8		12·2
416	−2·6		1·7		12·0
423	0·6		9·7		0·0
429	2·4	47	0·9	48	14·9
432	3·6		1·4		15·8
439	−1·6		2·7		13·4
443	4·6		2·9		7·6

Table X. Seismic Foci in Region IV.

No. of Earthq.	X	No. of Fig.	Y	No. of Fig.	Focal Depth.
	km.		km.		km.
1	19·6		3·3		15·5
3	18·7		1·6		19·3
4	12·8		− 4·8		20·3
6	18·5		−13·0		11·2
7	18·5		−13·0		11·2
20	13·0		6·4		14·1
21	14·8		2·2		19·3
23	11·0		2·6		14·6
24	20·0		5·0		17·2
49	19·6		− 1·0		16·0
50	19·6		0·2		16·1
68	19·1		− 2·8		16·6
69	19·9		− 2·7		18·0
76	14·9		− 2·4		13·7
77	13·9		1·5		13·5
87	19·4		− 4·9		12·8
99	17·8		− 0·3		14·1
103	8·5	49	3·2		19·9
114	19·6		− 4·0	53	20·5
116	19·5		− 3·3		17·1
118	15·9		− 2·0		19·5
120	17·4		7·4		19·2
121	17·7		1·2		19·2
146	15·8		− 0·6		11·4
152	18·7		− 8·0		0·0
155	15·8		0·1		14·0
161	5·6		6·6		16·4
174	19·0		0·6		16·7
177	14·1		5·7		19·3
186	11·7		7·0		21·4
187	9·4		2·2		17·8
188	9·4		2·2		17·8
189	5·1		3·8		18·4
190	3·5		3·7		18·8
191	2·9		2·7		17·2

(*to be continued.*)

Table X. (*continued.*)

No. of Earthq.	X	No. of Fig.	Y	No. of Fig.	Focal Depth.
	km.		km.		km.
192	10·5	49	−0·6	54	20·2
199	19·5		−4·6		16·9
201	13·8		−3·2		17·0
202	15·2		−5·1		13·6
204	11·9		−2·4		15·2
205	12·2		1·7		13·8
206	12·0		2·8		15·1
207	15·0		−4·0		15·5
210	8·4		−1·8		15·4
211	12·3		0·9		18·2
212	11·6		−5·2		13·6
213	13·3		−4·3		13·5
214	9·1		−5·5		16·2
215	10·3		−5·6		14·5
219	4·5		0·6		17·1
221	11·3		−2·6		17·8
222	11·9		−4·2		16·9
224	16·8		3·8	54	20·8
225	11·9		5·0		18·7
226	19·0	50	−0·6		16·6
231	13·9		1·4		21·2
233	11·9		1·5		17·4
234	19·1		−2·9		16·4
237	19·2		−5·3		9·4
240	17·2		−1·7		18·5
243	2·6		3·2		19·0
246	18·2		2·1		18·7
253	2·8		−0·6		17·4
255	13·5		−4·8		14·3
272	19·1		−2·9		16·4
275	19·8		0·4		9·6
285	16·5		1·5		13·0
296	8·6		4·6		17·8
299	18·5		4·8		16·6
305	1·2		−3·6		11·2
307	18·2		11·6		21·5
308	15·0		4·3		15·4
319	16·0		3·6		15·8
320	10·7		1·9		14·0
322	19·5		7·9		15·5
328	11·0		5·0		16·4
351	16·0		−3·7	55	15·7
361	9·4		6·8		16·6
370	15·1		6·8		16·8
371	15·1	51	6·8		16·8
385	19·1		−5·2		15·7
394	13·7		6·2		7·8
398	19·0		−1·1		12·4
399	20·0		−5·2		11·6
408	17·4		5·0		9·1
409	19·1		−1·8		6·6

28. 昭和2年丹後大地震の餘震の震原立體分布に關する研究補遺

地震研究所　那　須　信　治

丹後地震の餘震觀測報告（東京帝國大學理學部紀要，[ii]，**3**（1929），29～129 及び地震研究所彙報 **6**（1929），245 及び **7**（1929），133 に記載）が出版された後震原の立體分布に就いて補足及び訂正を要する箇所があることを認め此論文には主として此等の點が取扱はれてゐる．卽ち主なる補足訂正の點は次の通りである．

（1） 距離係數 k を計算により小數第2位まで求めた．但し前回の報告中8の地震に就いて k を求めたものをこゝでは9の地震に就いて求めた．此の計算の結果平均 $k=8{\cdot}40$ となり，前回の $k=8{\cdot}41$ とは僅かに 0·01 の差があることを見出した．本論文中の震原位置決定には 8·40 の値が採用されてある．又前に發表した表（理學部紀要 [ii]，**3**（1929），38，Table V；震研彙報 **6**（1929），257，Table III）は筆者が實地に測定せざる觀測資料を含み尙ほ不合理と思はれる點もあるので此表は除外することにした．

（2） 前報告中の震原の中約 30 箇は不確實と思はれるので，此論文中では此等の震原を除外した．

（3） 震原位置の誤差は地震の起る弱線の配列を論ずるに十分な程度に精密に計算したが，此處では計算を記載することを省略し必要に應じてその結果のみを引用した．

（4） 前に發表した報告中の震原立體分布圖の中で震原の乘る線を餘りに多數引き過ぎた傾向があつたが，震原位置の誤差を考へるときは實在性が疑はれるやうなものがあつたので本論文中には最も實在し得ると考へられたものゝみを指摘した．

（5） 地震の活動中心の移動を適確に示すために地震を發震日時の順によつて區分したがその區分を前回に報告した時よりは細密に行つて結果は概して良好の樣に思はれた．

其他細部に亘る訂正補足は尙ほ數箇條あるが全般を貫く大綱に到つては前回の報告中に述べたものと大差はない．